Meteoritics & Planetary Science 39, Nr 6, 879–897 (2004)
Abstract available online at http://meteoritics.org

Impact lithologies and their emplacement in the Chicxulub impact crater: Initial results from the Chicxulub Scientific Drilling Project, Yaxcopoil, Mexico

David A. KRING,[1*] Friedrich HÖRZ,[2] Lukas ZURCHER,[1] and Jaime URRUTIA FUCUGAUCHI[3]

[1]Lunar and Planetary Laboratory, University of Arizona, 1629 East University Boulevard, Tucson, Arizona 85721, USA
[2]Planetary Sciences Branch, SN2, NASA Johnson Space Center, Houston, Texas 77058, USA
[3]Instituto de Geofísica, Universidad Nacional Autónoma de México, Ciudad Universitaria, Mexico City 04510, Mexico
[*]Corresponding author. E-mail: kring@lpl.arizona.edu

(Received 3 September 2003; revision accepted 5 April 2004)

Abstract–The Chicxulub Scientific Drilling Project (CSDP), Mexico, produced a continuous core of material from depths of 404 to 1511 m in the Yaxcopoil-1 (Yax-1) borehole, revealing (top to bottom) Tertiary marine sediments, polymict breccias, an impact melt unit, and one or more blocks of Cretaceous target sediments that are crosscut with impact-generated dikes, in a region that lies between the peak ring and final crater rim. The impact melt and breccias in the Yax-1 borehole are 100 m thick, which is approximately 1/5 the thickness of breccias and melts exposed in the Yucatán-6 exploration hole, which is also thought to be located between the peak ring and final rim of the Chicxulub crater. The sequence and composition of impact melts and breccias are grossly similar to those in the Yucatán-6 hole. Compared to breccias in other impact craters, the Chicxulub breccias are incredibly rich in silicate melt fragments (up to 84% versus 30 to 50%, for example, in the Ries). The melt in the Yax-1 hole was produced largely from the silicate basement lithologies that lie beneath a 3 km- thick carbonate platform in the target area. Small amounts of immiscible molten carbonate were ejected with the silicate melt, and clastic carbonate often forms the matrix of the polymict breccias. The melt unit appears to have been deposited while molten but brecciated after solidification. The melt fragments in the polymict breccias appear to have solidified in flight, before deposition, and fractured during transport and deposition.

THE CHICXULUB IMPACT CRATER

The Chicxulub impact crater is a subsurface and partially submerged structure, so any direct analysis of the crater must rely heavily on drilling operations. After identifying nearly circular geophysical anomalies during oil surveys in the late 1940s (Cornejo Toledo and Hernandez Osuna 1950), several exploratory wells were drilled by Petroleos Mexicanos (PEMEX) in and around the structure. Three of the boreholes (Yucatán-6, Chicxulub-1, and Sacapuc-1) penetrated an aphanitic melt rock that was interpreted to be an extrusive (volcanic) andesite (Guzmán and Mina 1952; López-Ramos 1975) of Late Cretaceous age based on stratigraphic context.

Further examination of samples from the Yucatán-6 borehole, however, revealed shocked quartz in a polymict breccia that overlays a thick melt unit in the interior of the structure, indicating that the Chicxulub structure is an impact crater (Kring et al. 1991; Hildebrand et al. 1991). Other circumstantial evidence supported an impact origin. In particular, gravity and magnetic anomalies were consistent with an impact crater of that size (Penfield and Camargo-Zanoguera 1981, 1991; Hildebrand et al. 1991). The impact also penetrated Ca-carbonate and Ca-sulfate deposits, which were attractive sources for unusually calcic impact glasses found at K/T boundary sequences in Haiti (Sigurdsson et al. 1991a, b; Kring and Boynton 1991; Hildebrand et al. 1991).

An impact origin was rapidly confirmed in several other reports. It was shown that the composition of the melt rock below the polymict breccia in the Yucatán-6 borehole could not have been produced by volcanic processes but was, instead, produced by complete melting of the crustal basement at the point of impact (Kring and Boynton 1992). Relic shocked quartz clasts were found in the unit of melt rock (Hildebrand et al. 1992). It was also shown that the thickness of the K/T boundary impact ejecta in the North American region decreased with distance, as one would expect if it had been ejected from the Chicxulub structure (Hildebrand and Stansberry 1992; Vickery et al. 1992). The measured age of the Chicxulub melt rock (64.98 ± 0.05 Ma and 65.2 ± 0.4 Ma) was found to be the same as that of impact melt spherules (65.01 ± 0.08 Ma) deposited in a K/T boundary unit in Haiti (Swisher et al. 1992; Sharpton et al. 1992). The strontium and

oxygen isotopic compositions of impact melt spherules in K/T boundary sediments in Haiti were found to be consistent with a mixture of the Chicxulub melt rock and a K/T marine carbonate (Blum and Chamberlain 1992; Blum et al. 1993).

Although samples from the Yucatán-6 borehole were sufficient to demonstrate that the Chicxulub structure is an impact crater and the source of debris in K/T boundary sediments, there was not enough material to resolve several major questions, including fundamentally important issues involving the formation and detailed structure of a large scale peak ring crater and, possibly, multi-ring basin. Because Yucatán-6 (Fig. 1) was an oil exploration borehole, only about 1 m of sample was recovered for each 100 m of depth, and much of that material has been lost. The same situation exists for two other exploration boreholes drilled within the rim of the structure (Chicxulub-1 and Sacapuc-1) and five boreholes drilled outside the structure (Ticul-1, Yucatán-1, -2, -4, and 5a; see Fig. 1 inset). To remedy this problem, several additional wells with continuous core were needed. The first effort to obtain such cores was initiated by the Universidad Nacional Autónoma de México (UNAM), which began a shallow drilling program that has recovered additional samples of impact breccias in 3 boreholes outside the rim of the crater. Recovery depths range from ~60 m to ~700 m (e.g., Urrutia-Fucugauchi et al. 1996; Sharpton et al. 1999). However, several deep boreholes are still needed to penetrate the impact melt lithologies and underlying fractured target lithologies within the rim of the crater. The first of these is called the Chicxulub Scientific Drilling Project (CSDP) (Dressler et al. 2003a), which was drilled as part of the International Continental Drilling Program (ICDP) in a coordinated effort with UNAM.

CHICXULUB SCIENTIFIC DRILLING PROJECT (CSDP)

The CSDP was designed to recover continuous core in a location that samples a complete sequence of impact lithologies and bottoms in underlying fractured target rocks. Such deep, continuous core potentially can allow investigators to determine: 1) the morphology, internal structure, and thermal history of the impact melt sheet; 2) how the melt volume scales to the size of the crater; 3) any chemical and mineralogical heterogeneity and possible magmatic differentiation in the impact melt sheet; 4) the types of lithologies involved in the impact event; 5) how that material was excavated, transported, mixed, and deposited in and around the impact crater; 6) the abundances of those target lithologies that can produce climatically active gases and, thus, affect the post-impact environment; 7) the extent and nature of the post-impact hydrothermal system; and 8) evaluate the biologic recovery in the Gulf of Mexico region. In addition, the crater is a useful probe of the Earth, so material in Chicxulub can be used to determine the composition and structure of the continental crust that is represented by the Maya block. In this study, we will describe the impact lithologies recovered by CSDP and address items 4 and 5. Other studies in this issue will address the remaining items.

The drilling site is located at Hacienda Yaxcopoil along Federal Highway 261 about 16 km south of Umán, Yucatán. This location is 60 to 65 km from the center of the Chicxulub impact crater, or approximately 15 km beyond the transient (excavation) cavity, but is within the rim of the estimated ~90 km-radius final crater (Dressler et al. 2003a). The drilling site was cleared in early November 2001, and a well and pump to supply water to the drilling operation was installed. A base unit with an IDECO rotary rig was provided by PITSA (Perforaciones Industriales Termicas, S. A.), and a hybrid coring rig was provided by DOSECC (Drilling, Observation and Sampling of the Earth's Continental Crust, developed by NSF and the University of Hawaii). Drilling began on December 9, 2001. Because the crater is covered with Tertiary sediments, rapid and relatively inexpensive rotary methods were used for the first 404 m. It was estimated that cuttings up to 2 cm in diameter would be sampled over 2 m intervals at an estimated drilling rate of 5 to 8 m/hr. However, due to subsurface karst beginning at a depth of 13 m, cuttings were flushed into caves rather than being returned to the surface.

Rotary operations were completed on December 16, and logging of the upper 400 m was conducted using bedding dipmeter (TS-DIP), gamma-ray (TS-SGR-MS2H), and resistivity (TS-DLL) from depths of 0 to 402 m, and sonic velocity (BCS) in the upper 85 m. This portion of the hole was then cased while preparations were made to deploy the DOSECC top drive and wireline HQ drill string (producing a 63.5 mm- diameter core). Coring began on December 30, and continued 24 hr/day, 7 days/week until January 20, 2002 when the string became stuck at a depth of 993 m. The HQ string was left as casing, and a new NQ string (producing a 47.6 mm-diameter core) was inserted. Drilling continued from February 7 to February 24 when a resource-limited final depth of 1511 m was reached. Core recovery was 99% from 404 to 1511 meters.

As the recovered core was removed from the core barrel, it was washed clean, labeled, marked for orientation, and boxed. Core was moved at least daily to a temporary core laboratory at the Universidad Autónoma de Yucatán in Mérida where each core segment was briefly described and imaged with a rotating core scanner, and each core box was photographed. The impactite portion of the core was kept at a moderate temperature to avoid disturbing any fluid inclusions and causing Ar to degas. Temperatures were maintained below 40 to 50 °C (to remain below the homogenization temperature of trapped fluids and avoid Ar degassing) and well above 0 °C (to avoid freeze stretching of fluid inclusions). The material was then shipped to the CSDP core library at the Insituto de Geofísica and Instituto de Geología at UNAM in Mexico City for purposes of curation and sample allocation to international consortia and individual specialists.

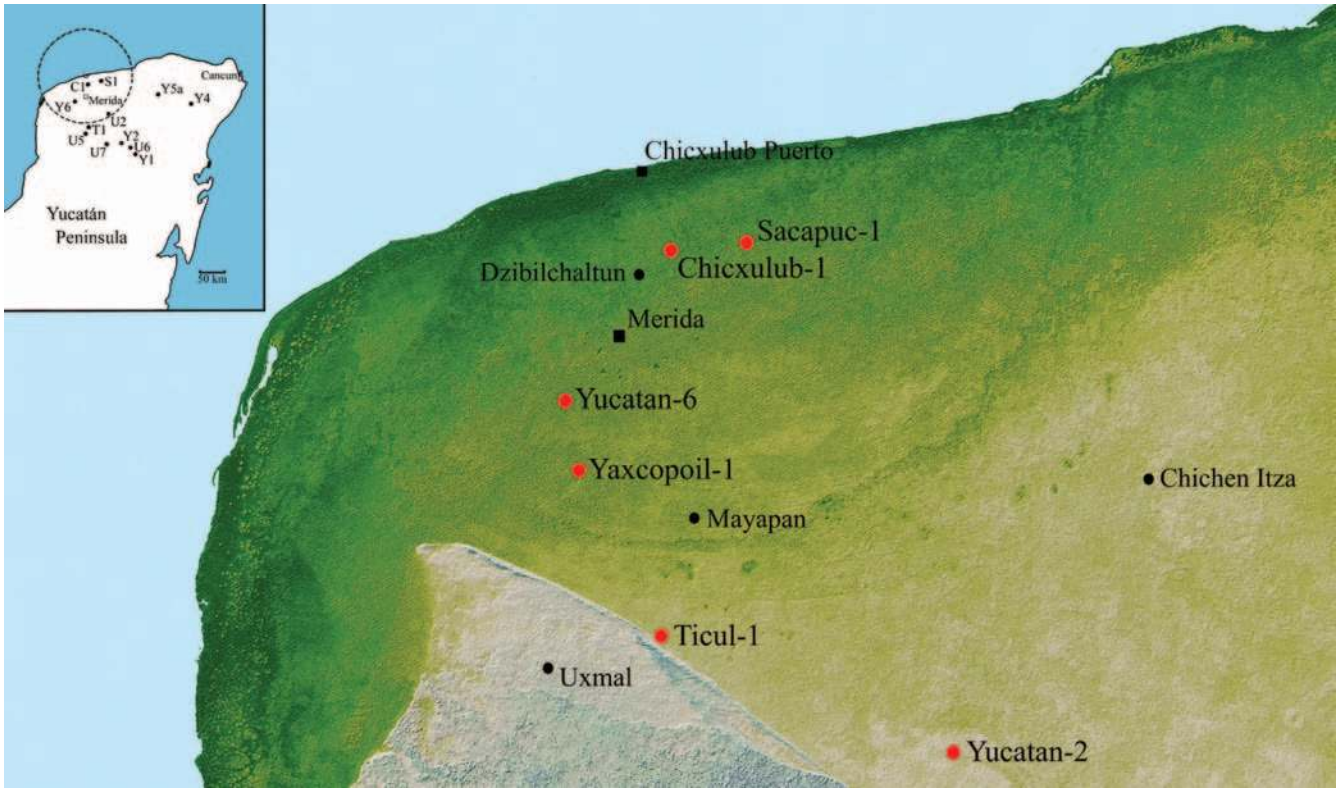

Fig. 1. Locations of exploration boreholes (red dots) in the vicinity of the Chicxulub impact crater on the Yucatán peninsula. The shaded relief map was produced by the Shuttle Radar Tomography Mission on Space Shuttle Endeavor in 2000. A 3–5 m deep semicircular trough (darker green arcing line) lies at a slightly smaller radius than a belt of cenotes which occur approximately above the crater rim. The Chicxulub-1, Sacapuc-1, Yucatán-6, and Yax-1 boreholes are within the rim of the crater. The original diagnostic evidence of shock-metamorphism and an impact origin for the structure was recovered from Yucatán-6 (Y6). All of the PEMEX exploration boreholes (C1, S1, T1, Y1, Y2, Y4, Y5a, Y6), which were often >1 km deep, were incompletely sampled (see inset). The newer UNAM exploration boreholes (U2, U5, U6, U7) recovered continuous core but are part of a shallow (ranging from ~60 m to ~700 m) drilling program. Only U5, U6, and U7 encountered impact lithologies. The dotted line in the inset outlines the ~170 to 180 km central region of the crater, which many investigators believe is the rim of the crater. The shaded relief image was produced by NASA, the National Imagery and Mapping Agency (NIMA) of the U.S. Department of Defense, and the German and Italian space agencies.

THE YAXCOPOIL-1 CORE

The Yax-1 core includes material from a depth of 404 m in Tertiary cover and goes through ~100 m of melt-bearing impactites between 794 and 895 m and 616 m of one or more blocks of Cretaceous target blocks before bottoming at 1511 m. Although hydrothermally altered (e.g., Zurcher and Kring 2004), the impactites are surprisingly competent, dense rocks that display well-preserved textural relationships. The on-site geologist, Burkard Dressler, logged 6 subunits within the impactite sequence, which were tentatively described from top to bottom as a redeposited suevite (unit 1, 13.39 m thick), suevite (unit 2, 14.86 m thick), chocolate-brown melt breccia (unit 3, 22.94 m thick), suevitic breccia (variegated and glass-rich) (unit 4, 15.26 m thick), green monomict autogene melt breccia (unit 5, 23.86 m thick), and variegated polymict allogenic-clast melt breccia (unit 6, 10.02 m thick) (Dressler et al. 2003a). Our preliminary analysis (Kring et al. 2003) suggested the impactite sequence is unusually rich in impact melts of a textural variety and complexity quite unlike melt-bearing impact formations from other terrestrial craters. Many other preliminary descriptions have also been published by other project scientists, and we refer readers to the published abstracts for the 34th Lunar and Planetary Science Conference, the EGS-AGU-EUG Joint Assembly, the 66th Annual Meteoritical Society Meeting, and the Third International Conference on Large Meteorite Impacts, all of which were held in 2003. Reports by Dressler et al. (2003b), Hecht et al. (2003), Kenkmann et al. (2003a, b), Schmitt et al. (2003a, b), Stöffler et al. (2003a, b, c), Tuchscherer et al. (2003), and Wittmann et al. (2003a, b) are particularly relevant to the issues explored in this study.

METHODS

After examining a ~100 m length of core through the impactite sequence plus underlying sections of core that are cross-cut by dikes, we selected a subset of samples for additional geochemical, isotopic, and petrologic studies. The standard sample sizes for CSDP are quarter-round sections of

the core that are 2 cm thick, and we were limited by the project to an initial set of 25 samples; twelve of those samples were studied in detail for this report (Table 1). Thin sections were prepared for petrological analyses using optical microscopy and electron microprobe techniques. Chemical analyses were obtained using a CAMECA SX-50 electron microprobe at the University of Arizona. The accelerating voltage was 15 keV, the beam current was 20 nA, and the beam diameter was <~1 μm. The calibration standards were a Fo_{90} olivine (Si; USNM 111312), natural fayalite (Fe; Rockport, Massachusetts), synthetic diopside glass (Mg; Boyd), natural anorthite (Al; USNM 137041), natural orthoclase (K; Penn State), natural albite (Na; Crete), natural wollastonite (Ca; C. M. Taylor Inc.), natural rhodonite (Mn; Minas Geras, Brazil), natural rutile (Ti; Arizona State University), natural chromite (Cr; USNM 117075), synthetic Ni-bearing diopside glass (Ni; D. Lindstrom), natural apatite (P; Durango, Colorado), synthetic Ba-rich silicate glass (Ba; NBS K458), natural sodalite (Cl; University of Arizona), synthetic MgF (F; Optovac Inc.), barite (S; C. M. Taylor Inc.), and vanadium metal (V).

Table 1. Yax-1 samples included in this study and their depth in the core.

Sample label	Sample depth (m)	Corresponding unit[a]
Yax-1_800.43	800.43	1
Yax-1_819.83	819.83	2
Yax-1_829.56	829.56	3
Yax-1_831.345	831.345	3
Yax-1_836.34	836.34	3
Yax-1_841.32	841.32	3
Yax-1_857.65	857.65	4
Yax-1_861.4	861.4	5
Yax-1_863.51	863.51	5
Yax-1_876.46	876.46	5
Yax-1_883.13	883.13	5
Yax-1_1398.53	1398.53	Below 6

[a]As described by Dressler et al. (2003a).

RESULTS

Lithological Descriptions

Like the Yucatán-6 material (Kring et al. 1991; Hildebrand et al. 1991; Claeys et al. 2003), the impactites in the Yax-1 core are composed of an upper sequence of polymict melt-bearing impact breccias and a basal melt unit. However, while the Yucatán-6 borehole only provided intermittent samples as a function of depth, the Yax-1 core provides a continuous sample of the impactite sequence and, thus, a more complete record of the impact deposits.

Impact Melt

A coherent 24 m-thick green impact melt lies near the base of the impactite sequence above one or more megablocks of target sediments. Thus far, we have examined four samples from the top to the bottom of this green melt zone: Yax-1_861.4, Yax-1_863.51, Yax-1_876.46, and Yax-1_883.13, where the numbers following Yax-1 indicate the depth of the samples in meters. The green melt is generally massive in appearance (Figs. 2–3), but contains flow lines on both macroscopic and microscopic scales that are suggestive of incompletely mixed and rapidly quenched melt. However, the melt is aphanitic (Fig. 4), and no fresh glasses were observed. The melt is dominated by microcrystalline (2–50 μm), Ca-rich pyroxene ($Wo_{46–50}En_{41–35}Fs_{11–15}$), plagioclase ($An_{36–58}Ab_{60–40}Or_{2–9}$), and alkali feldspar ($An_{0–12}$ $Ab_{98–9}Or_{2–90}$) (Table 2). The Yax-1 melt is slightly coarser than the melt in the Yucatán-6 borehole (2–10 μm; Kring and Boynton 1992). However, pyroxene and plagioclase compositions (Fig. 5) are similar to those in the melt recovered from the Yucatán-6 borehole (Kring et al. 1991; Hildebrand et al. 1991; Kring and Boynton 1992). The Yax-1 green melt also contains primary apatite, primary and secondary magnetite, rutile (or secondary anatase), secondary barite, secondary calcite, and secondary phyllosilicates. In this unit, as in all other units, secondary phases are identified on the basis of texture (i.e., they are replacing primary minerals, fill cavities, or occur in veins). In the core, granitic clasts up to 4.5 cm and mafic clasts up to 6.5 cm were observed. In thin section, small amounts of shocked and unshocked clasts are entrained in the melt, including quartz and quartzite with planar deformation features and ballen structures after cristobalite (Fig. 4b), isolated altered feldspar and mafic minerals, and mafic lithics.

These clasts are <0.5 cm in the longest dimension and comprise 2–4% of a thin section, depending on the sample. The abundance of xenocrysts and xenoliths in the melt is comparable to that (2%) in the Yucatán-6 melt unit (Kring and Boynton 1992). Inclusions within the thin section are aligned, as in a trachytic texture, implying that the melt was flowing before solidification.

The green melt is also brecciated and highly altered along its margins where the contacts were conduits for carbonate-rich fluids. While the core was being recovered, a 10 m-thick carbonate-charged and brecciated green impact melt unit (unit 6) with larger clasts of target material, including a 34 cm granite, was logged below the principal 24 m-thick green melt unit (unit 5). As discussed in greater detail below, this may be the basal, more disaggregated portion of the green melt unit, rather than a depositionally distinct melt unit. Secondary hydrothermal veins that crosscut this unit have themselves been offset by fracturing within the unit (Zurcher and Kring 2004). This implies some of the brecciation that affected the melt unit occurred after the formation of at least some hydrothermal veins and not during the depositional process.

Polymict Impact Breccias

Above the green melt unit are a series of melt-rich breccias that are an unusual agglomerate of melt clasts, ranging from distinctly brittle melt fragments to flowed

Table 2. Representative microprobe analyses of pyroxene, plagioclase, apatite, sphene, and Fe-Ti-oxide.

	Yax-1	Yax-1	Yax-1	Yax-1	Yax-1	Yax-1	Yax-1	Yax-1	Yax-1	Yax-1
Wt%	863.51	861.40	872.32	863.51	861.40	883.13	883.13	836.34	832.83	836.34
Oxide	Unit 5	Unit 5	Unit 5	Unit 5	Unit 5	Unit 6	Unit 6	Unit 3	Unit 3	Unit 3
	Pyx	Pyx	Plag	Plag	Plag	Apat	Apat	Apat	Sphene	Fe-Ti-ox
SiO_2	51.69	51.90	55.45	54.61	55.67	0.58	0.39	0.08	30.07	0.17
TiO_2	0.43	0.41	0.06	0.07	0.05	0.01	0.04	n.d.	38.36	5.56
Al_2O_3	3.10	3.02	26.61	27.31	26.57	0.01	0.01	n.d.	1.27	2.20
Cr_2O_3	0.03	0.01	n.d.	0.04	0.01	n.d.	n.d.	n.d.	n.d.	0.02
MnO	0.18	0.17	0.04	0.02	0.03	0.07	0.04	0.05	0.10	0.28
FeOT[a]	6.90	7.22	1.23	1.53	1.76	0.34	0.36	0.09	0.98	–
FeO_{calc}[b]	–	–	–	–	–	–	–	–	–	27.64
Fe_2O_{3calc}[b]	–	–	–	–	–	–	–	–	–	61.44
NiO	0.03	n.d.	0.02	n.d.	n.d.	n.d.	0.04	n.d.	0.01	0.06
MgO	13.76	13.77	0.18	0.17	0.30	0.31	0.24	n.d.	n.d.	1.62
CaO	23.67	23.55	9.74	10.94	10.37	53.05	52.88	57.19	28.08	0.04
Na_2O	0.42	0.43	5.50	5.07	5.28	0.51	0.64	0.04	0.03	0.02
K_2O	0.06	0.08	0.57	0.37	0.47	0.12	0.05	0.01	0.04	0.04
P_2O5	0.05	0.07	n.d.	n.d.	n.d.	38.60	38.02	40.50	0.03	n.d.
F	0.13	n.d.	0.02	n.d.	n.d.	5.54[c]	4.00[c]	n.d.	0.32	0.04
Cl	0.01	0.02	0.02	0.01	0.01	0.86	0.83	0.02	n.d.	0.01
S	n.d.	n.d.	n.d.	0.01	n.d.	0.42	0.50	0.03	n.d.	0.01
Total	100.46	100.65	99.44	100.15	100.52	100.42	98.04	98.01	99.29	99.15
Ae	1.5	1.6	–	–	–	–	–	–	–	–
Wo	48.4	47.9	–	–	–	–	–	–	–	–
En	39.1	39.0	–	–	–	–	–	–	–	–
Fs	11.0	11.5	–	–	–	–	–	–	–	–
An	–	–	47.8	53.2	50.6	–	–	–	–	–
Ab	–	–	48.9	44.6	46.7	–	–	–	–	–
Or	–	–	3.3	2.2	2.7	–	–	–	–	–

[a]Fe measured as FeO.

[b]Measured Fe recalculated as FeO and Fe_2O_3.

[c]These values are spuriously high because of diffusion during the analyses.

bodies. A 15 m-thick breccia (unit 4) was logged immediately above the green melt unit with abundant and sometimes very large (up to 20 cm) clasts of banded melts (Fig. 2). In sample Yax-1_857.65 (Figs. 2 and 3), the melt is dominated by microcrystalline (<20 μm), pyroxene ($Wo_{46–51}En_{43–37}Fs_{10–13}$), plagioclase ($An_{48–56}Ab_{48–41}Or_{5–2}$), and alkali feldspar ($An_{0–9}Ab_{1–42}Or_{49–99}$), with minor apatite, primary and secondary magnetite, secondary ilmenite, and rutile (or secondary anatase), similar to the green melt, although the color (shades of rose) is different. The melt entrained small amounts of shocked and unshocked clasts of quartz, feldspar, sandstone, metaquartzite, and granite. These melt fragments exist in a breccia that is variously clast and matrix supported, the latter of which appears to have been a conduit for post-impact fluids and is now charged with secondary alkali feldspar and subordinate carbonate.

A 23 m-thick melt-rich breccia (unit 3) is next in the sequence (Figs. 2 and 3), which we examined in Yax-1_829.56, 831.345, 836.34, and 841.32. This unit is dominated (up to 84%; Table 2) by fragments of altered (see Zurcher and Kring 2004) silicate impact melt (Fig. 6), generally with microcrystalline textures (<10 μm equant pyroxene, <50 μm long feldspar needles), although some fragments appear to have been partly to wholly glassy before being replaced by phyllosilicates and calcite. Primary minerals in the microcrystalline melts include pyroxene ($Wo_{48–51}En_{42–35}Fs_{10–14}$), plagioclase ($An_{50–59}Ab_{39–45}Or_{2–5}$), alkali feldspar ($An_{0–1}Ab_{0–10}Or_{100–88}$ and $An_5Ab_{94}Or_1$), magnetite, and Fe, Ti-oxides. Some of these silicate melts contained immiscible carbonate melt, gas vesicles (some of which were subsequently filled with secondary calcite and silicates), and flow-aligned crystals. In general, these melt fragments are more vesicular than those in the stratigraphically overlying suevitic units (described below). One clast has an aerodynamic morphology. The melt fragments in this breccia section (unit 3) entrained feldspar, quartz, magnetite, armalcolite-sphene assemblages, lithic metaquartzites, micritic carbonate, shale, and crystalline mafics.

The textural distinction between solidified silicate melt with immiscible carbonate melt and solidified silicate melt with gas vesicles subsequently filled with calcite is subtle. Ellipsoids of carbonate protruding from the edges of silicate melt fragments into the breccia matrix indicate that the carbonate was solid before the fragmentation of the melt fragment and incorporation into the breccia. In this case, the

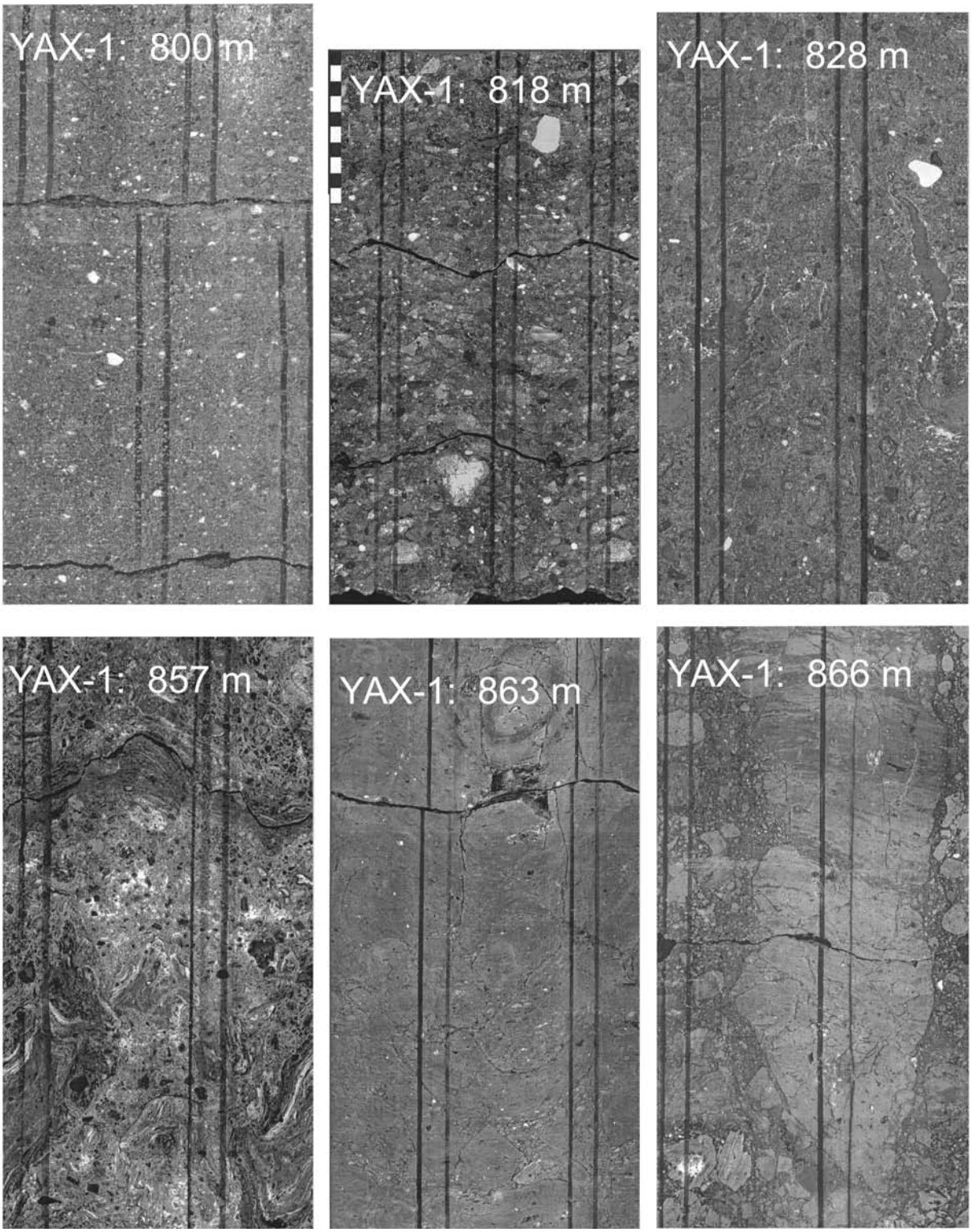

Fig. 2. Yax-1 core segments of polymict impact breccias and impact melt units. These are full 360° scans, so the width of each image corresponds to the circumference (20 cm) of each 63.5 mm diameter core. These images represent units 1 (800 m), 2 (818 m), 3 (828 m), 4 (857 m), 5 (863 m), and a second, more brecciated portion of 5 (866 m). Units 1 and 2 are poorly sorted clastic polymict breccias, although clast sizes in unit 1 are typically smaller than those in unit 2, producing a normally graded sequence. Unit 3 is also a clastic breccia, but it also contains large fluidal solidified melt fragments. Unit 4 contains large melt fragments with schlieren in a clastic matrix that is charged with secondary (hydrothermal) carbonate precipitates. Unit 5 is a coherent green melt unit that was brecciated after solidification. The vertical lines on the cores were drawn on them when the cores came out of the ground to mark proper orientation.

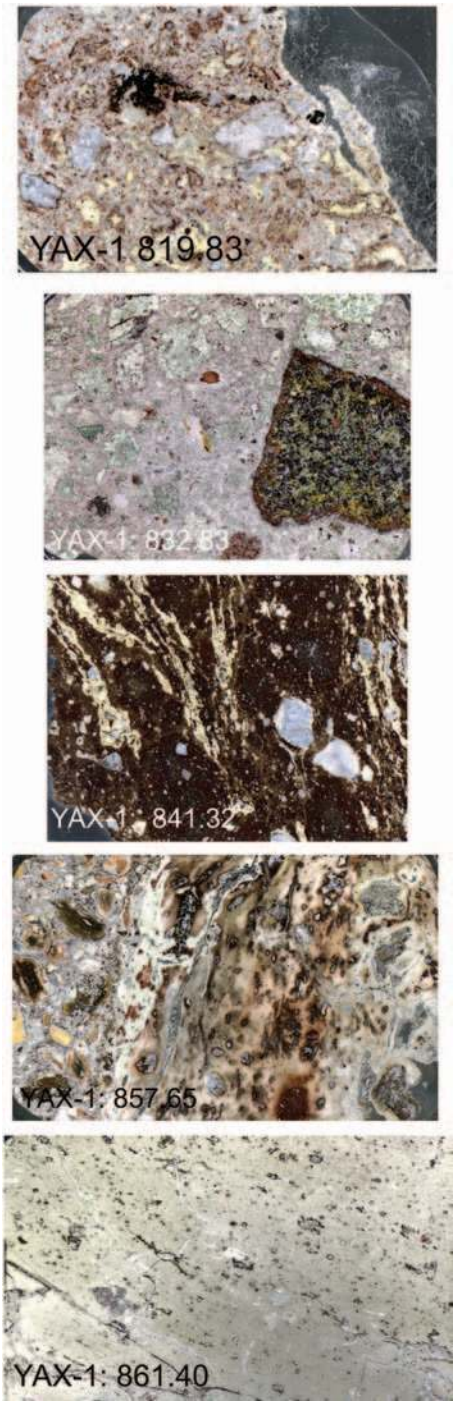

Fig. 3. Thin section views of the impactite sequence: unit 2 (819.83 m), unit 3 (832.83 m), an altered, brown melt sample in unit 3 (841.32 m), unit 4 (857.65 m), and unit 5 (861.40 m). Units 2 and 3 are dominated by fragments of splintered melt, although they also contain relict clasts of target lithologies that have been variously shock-metamorphosed. Units 3 and 4 have large fragments of impact melt with schlieren. In the case of unit 3, the entire 841.32 m thin section is melt. In the case of unit 4, the melt is in the center and right-hand side of the image. The matrix adjacent to the clast is in the left-hand side of the image. Unit 5 is a coherent, altered melt, with a flow fabric and small inclusions of unmelted target material. The widths of the images are 3.0, 2.8, 2.8, 3.3, and 3.2 cm, respectively.

Table 3. Proportions of clasts and matrix in Yax-1 polymict breccias.[a]

	Yax-1 836.34 Unit 3	Yax-1 832.83 Unit 3	Yax-1 829.56 Unit 3	Yax-1 819.83 Unit 2
Melt fragments	49(66)[b]	59(73)[b]	84	70(81)[c]
Crystalline clasts	26(0)[b]	24(6)[b]	<1	<1(<1)[c]
Sedimentary clasts	<1(1)[b]	1(1)[b]	n.d.	n.d.
Calcite matrix	24(33)[b]	16(19)[b]	10	16(19)[c]
Phyllosilicate matrix	n.d.	n.d.	6	n.d.
Secondary veins	1(1)[b]	n.d.	n.d.	14(0)[c]

[a]Unit 4 is excluded because it is too coarse for meaningful proportions to be obtained in thin section; measurements will need to be made directly in the core; unit 1 was not included in the first set of thin sections.
[b]Values in parentheses exclude a large mafic clast in the thin section.
[c]Values in parentheses exclude a large secondary vein in the thin section.

carbonate is a primary phase and was immiscible when the melts were molten. Ellipsoids of carbonate completely bounded by silicate melt could also represent immiscible carbonate melt but, in these cases, could instead be ellipsoids of secondary carbonate filling gas-evacuated vesicles.

Parts of the unit are clast supported, although the amount of matrix appears to increase from ~15 to ~24% (possibly 33%) with depth (Table 3); additional samples throughout this portion of the core will be needed to determine if this trend is real. The matrix is composed of calcite, an altered silicate phase, and magnetite. The altered silicate phase is more abundant higher in the section, so if it represents fine-grain melt particles (glass), there was more of it in the upper part of the unit. The large melt fragments have several different colors. Some green melt fragments, similar, if not identical, to the green melt unit below, are up to 17 cm long (see the sample from 828 m in Fig. 2). Brown melt samples have microcrystalline textures, schlieren, and clasts of shocked target lithologies. In one case, green melt surrounds a black melt fragment which, in turn, encloses a granitic inclusion. Mineralogically, the different-colored microcrystalline melts look the same (as seen through the haze of alteration) and also resemble the melts in the Yucatán-6 borehole. The colors may be a consequence of variable iron oxidation or the presence of phyllosilicates and other secondary minerals rather than large chemical variation in melt compositions. For example, the green melt fragments contain secondary chlorite, the brown melt fragments contain secondary carbonate, and the rose-colored melt fragment described above contains secondary potassium feldspar. The base of this unit is charged with carbonate, and it appears that the contact between the units was a fluid conduit.

Above this unit is a 15 m-thick unit (Figs. 2 and 3) that was logged as a suevite (unit 2), which we examined in sample Yax-1_819.83. This unit has a variety of sedimentary and crystalline clasts up to 7 cm but is dominated (81%; Table 2) by silicate melt fragments. The smallest melt fragments are mostly 100 to 150 μm and the largest melt fragment in our

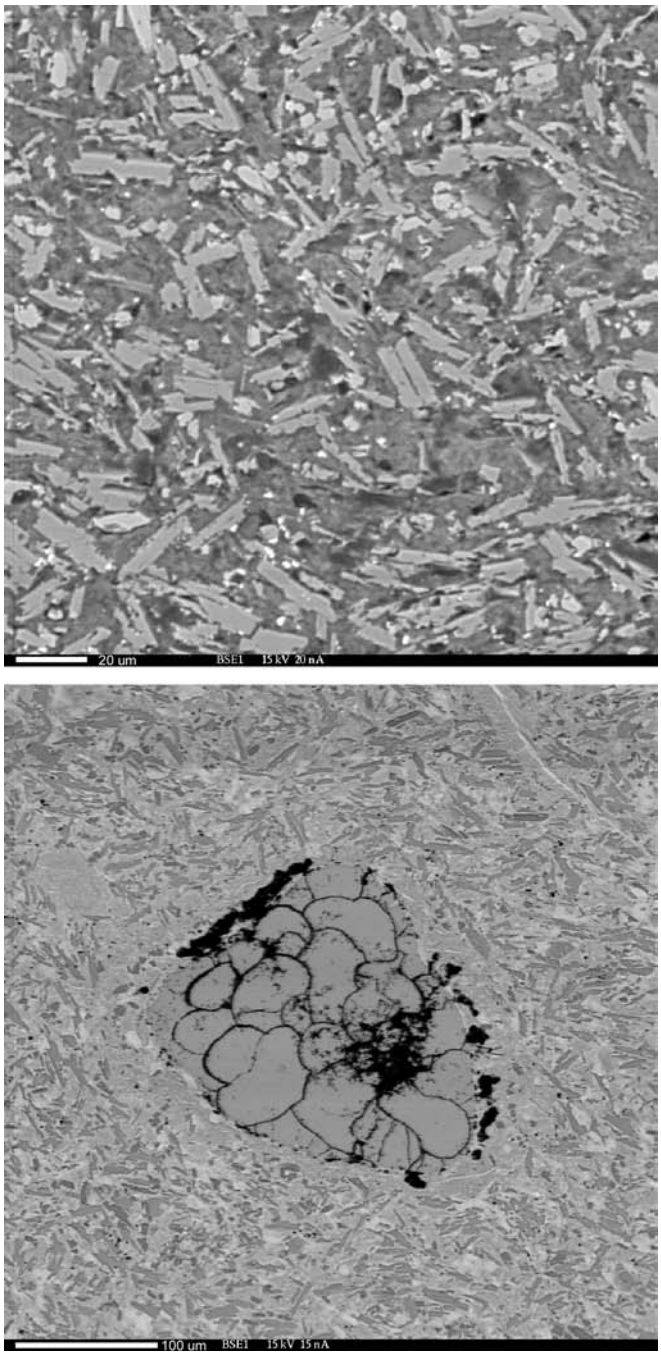

Fig. 4. Backscattered electron images of the green melt unit (5): a) groundmass with plagioclase, rare pyroxene (due to alteration), magnetite, and phyllosilicates (after glass?). Scale bar = 20 μm; b) lithic silica clast, with ballen structure indicative of shock-metamorphic cristobalite, within the pyroxene and plagioclase groundmass of the green melt unit. Scale bar = 100 μm.

collection is 1.4 cm. The matrix is composed of calcite that may have subsequently recrystallized and only comprises 19% of Yax-1_819.83. The matrix does not have the phyllosilicate component seen in unit 3. Secondary carbonate permeates portions of the matrix and fills a 7 cm cavity.

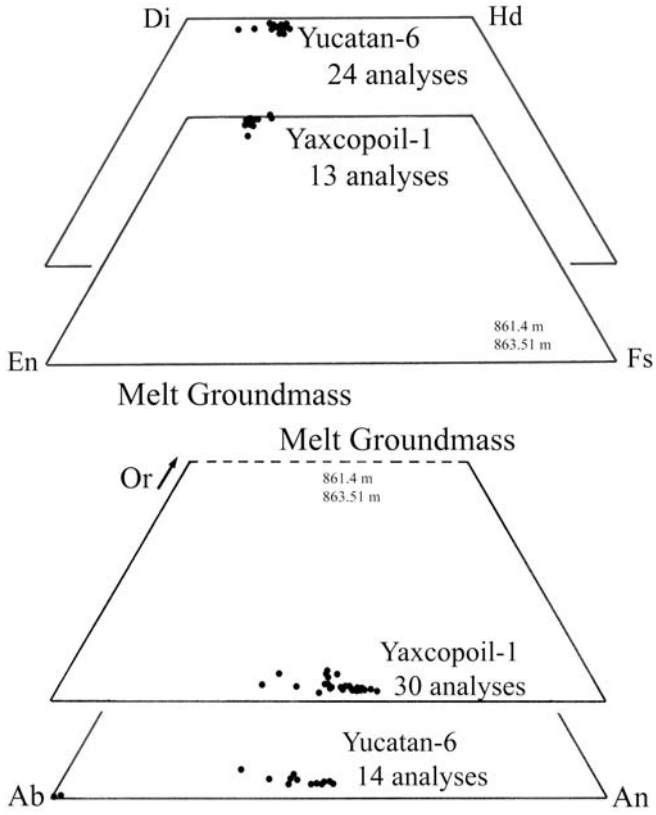

Fig. 5. Compositions of pyroxene and feldspar in the groundmass of the Yax-1 green melt unit (5) compared to similar compositions in the Yucatán-6 borehole. The unit (5) samples are Yax-1_861.4 and Yax-1_863.51. The Yucatán-6 sample is Y6N17 (see Kring and Boynton [1992] for more details).

The uppermost impact unit is 13 m thick (unit 1; Fig. 2) and is logged as a suevite. Our observations (see also Dressler et al. 2003) indicate that it is a finer-grained version of the material in unit 2 that has been reworked, presumably by currents on the sea that filled the crater, possibly induced by the impact. Our microscopic analyses are limited thus far to a 2 cm-wide calcite vein in sample Yax-1_800.43, which we also analyzed in the context of post-impact hydrothermal activity (Zurcher and Kring 2004; Zurcher et al. 2004). This sample is mainly a coarse unconsolidated sediment, with particle sizes <3 mm.

Dikes in Underlying Megablocks

Beneath the impactites are lithologically diverse megablocks composed of limestone, dolomite, and anhydrite, which are the dominant near-surface lithologies of the Chicxulub target. Melt and clastic dikes crosscut these Cretaceous megablocks, which are only modestly deformed yet of variable dip as detailed by Kenkmann et al. (2003a). We were unable to obtain a sample of a melt dike in our initial set of specimens but were able to study a clastic dike from a depth of 1398 m (Yax-1_1398.53). This is a small dike, stained black by hydrocarbons, that cuts a limestone block with microfaults

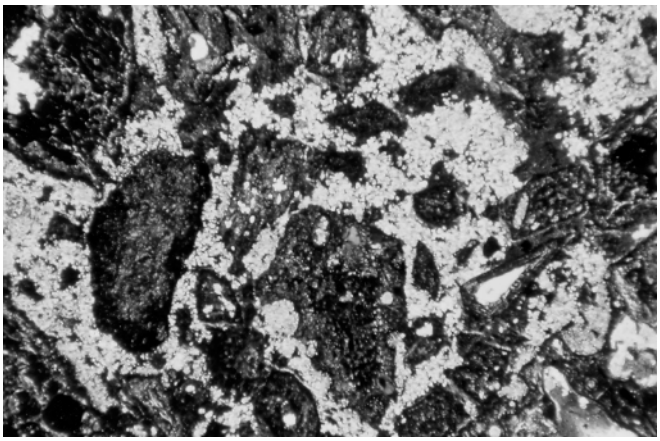

Fig. 6. Thin section view in cross polarized light of sample Yax-1_831.345 (unit 3), illustrating the large amount of silicate melt fragments (black shards) and small amount of carbonate matrix (light colored and recrystallized). Width = 2.4 mm.

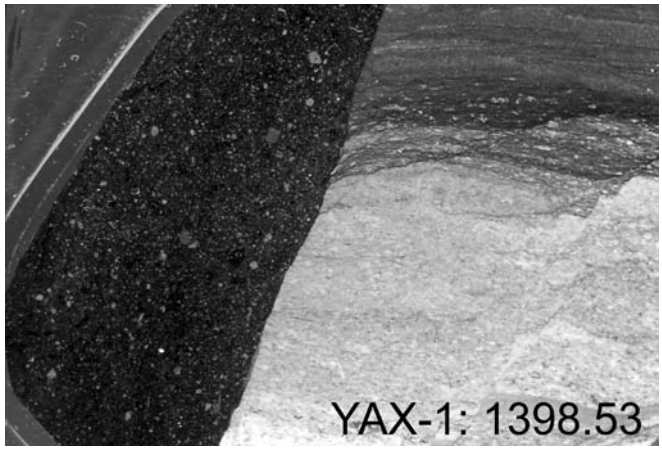

Fig. 7. Thin section view of a clastic dolomite-dominated and hydrocarbon-charged dike (left) that crosscuts a limestone megablock beneath the melt-rich impactite sequence (sample Yax-1_1398.53). The limestone is finely laminated (oriented horizontally in this image) and crosscut with normal microfaults (right). Hydrocarbons are migrating parallel to the laminations (top right) to the porous and permeable dike. The upper and lower left corners are epoxy-coated glass. Width = 3.1 cm.

(Fig. 7), similar to those described by Kenkmann et al. (2003a) and Wittmann et al. (2003a). The host limestone is a finely laminated, microfaulted, but essentially flat-lying unit that may be classified as a biomicrite due to the presence of fossil remnants and biogenic clasts.

The dike matrix is composed of dolomite (>95%) and minor limestone and anhydrite. The dolomite fragments are typically 100 μm in size or smaller, yet the dike includes somewhat larger, distinctly lithic clasts, most more coarse-grained than the matrix. The dike is, thus, a totally cataclastic dike substantially composed of finely pulverized dolomite. The contact relationships with the limestone wall rock are sharp and lack gradational disaggregation of the host. Nevertheless, a number of limestone clasts that could be associated with the host occur throughout the cataclastic dike matrix. Small amounts of extremely fine-grained FeS_x, most likely pyrite, and Fe-oxides occur in both the dike and the limestone host, as do minute orthoclase fragments. Anhydrite is also in the dike and concentrated along one margin.

Lithic dolomite clasts have variable grain size, suggesting that they are derived from several dolomite sources. While most limestone clasts are indistinguishable from the host, some individual calcite fragments are distinctly larger than anything observed in the host rock. Also, fragment size of the dolomite matrix varies locally, suggesting different degrees of cataclasis, including abrupt changes that suggest a "breccia within breccia" relationship. The latter is clearly the case for a large dolomite clast, which contains anhydrite in its interior.

In addition, it is also important to note that breccia pockets or large clasts of dolomite and anhydrite occur in the vicinity of these types of cataclastic dikes (e.g., at 1376 and 1399 m; Dressler, personal communication). The sources of the anhydrite and dolomite within the black dike at 1398.53 m is unclear but requires transport on the scale of at least meters into the limestone host. We also note that the original stratigraphic provenance of these sedimentary clasts is completely unknown at present, including the specific limestone host at 1398 m depth.

DISCUSSION

The Chicxulub structure is a complex peak ring crater and potentially a multi-ring basin that is buried beneath several hundred meters of Tertiary cover, making it difficult to determine transient and final crater rim diameters. The final crater rim diameter has been variously estimated to be from 130 to 300 km based on geophysical data, exploration borehole logs, and impact crater scaling relationships (e.g., Hildebrand et al. 1991, 1995; Sharpton et al. 1993; Camargo-Zanoguera and Suárez Reynoso 1994; Pilkington et al. 1994; Kring 1995; Morgan et al. 1997, 2000; Campos-Enríguez et al. 1997; Morgan and Warner 1999; Delgado-Rodríguez et al. 2001). Radially disparate well locations, difficulty tying onshore data with offshore data, and possible erosion of the crater rim have complicated these assessments. Final crater diameters in the range of 140 to 200 km are preferred by most investigators, corresponding to different changes in basin slope: one at ~130 to ~145 km and another at ~170 to ~200 km. A value of ~180 km is consistent with estimates from scaling relationships and gravity, magnetic, and magnetotelluric anomalies (see references above). The types of impactites and their thicknesses in Yax-1 are consistent with an approximate final crater diameter of this value rather than a substantially larger value of 250 to 300 km. An additional fault scarp with a diameter of ~250 km is visible in seismic data (Morgan et al. 1997) and may correspond to a gravity anomaly feature of ~300 diameter (Sharpton et al. 1993), in which case it would be an external fault scarp

characteristic of multi-ring basins (Kring 1995; Morgan and Warner 1999; Morgan et al. 2000).

The smaller transient crater diameter, corresponding to the dimensions of the zone of excavation, is currently estimated to be between ~90 and ~110 km (e.g., Pilkington et al. 1994; Kring 1995; Morgan et al. 1997, 1999), with a value of ~100 km cited most often.

The Yax-1 borehole is the fourth well to penetrate impact lithologies within the rim of the ~180 km-diameter Chicxulub crater. Two previous wells, Chicxulub-1 and Sacapuc-1, penetrated the polymict breccias and the central melt sheet within the peak ring. The Yucatán-6 well is near the peak ring. Seismic data obtained north of Yucatán-6, but rotated to the drill site assuming radial symmetry, suggests it is slightly outside the peak ring (J. Morgan, personal communication). The Yax-1 is still farther to the south and, based on our reconstruction of the crater, penetrates the trough between the peak ring and final rim (Figs. 1 and 8), which is consistent with offshore seismic data (Bell et al. 2004). The impactite sequence, thus, represents material formed in the transient crater and transported up to tens of km. We begin our discussion with an examination of the lithologies excavated from the target that are readily identifiable as clasts in the breccias. We then discuss the impact melts, which are mixtures of these and potentially other target lithologies.

Excavated Components

Surviving clasts of crystalline materials in the Yax-1 samples include isolated quartz, feldspar, magnetite, and altered mafic minerals and lithic clasts of granite-granodiorite, metaquartzite, shale, micritic limestone, and unidentified crystalline mafics. The siliceous, feldspathic, and carbonate lithologies are similar to those seen in the Yucatán-2, Yucatán-6, and Sacapuc-1 boreholes, where clasts of sedimentary carbonates and evaporites, recrystallized sandstones, granitic gneisses, and mica schists in a carbonate-rich matrix were identified (Kring et al. 1991; Hildebrand et al. 1991; Kring and Boynton 1992; Sharpton et al. 1992, 1996).

The mafic lithologies are new, however, although there were chemical and isotopic hints of mafic target components in the Yucatán-6 core. In mixing calculations using major and minor elements of the melt composition, a contribution from a mafic source like diabase, pyroxenite, or amphibolite was inferred (Kring and Boynton 1992). Traces of crustal spinel from an unidentified lithology were found in samples of K/T ejecta (Kring et al. 1994). Kettrup et al. (2000) measured Sm-Nd and Rb-Sr isotope compositions of several Chicxulub lithologies and also concluded that there was a mafic to intermediate component that had not been identified. It was clear that the mafic material was a crustal component and not a contribution from the mantle.

Unfortunately, post-impact hydrothermal activity (Zurcher and Kring 2004) has altered the mafic clasts we have studied thus far. A mafic clast in Yax_1_821.76, for example, has been almost completely converted to a clay-rich assemblage. Primary plagioclase microcrysts and a foliated rock texture can still be observed, and the clast is richer in apatite than the surrounding host breccia, but everything else is secondary (hydrothermal magnetite, quartz, calcite, chlorite, and clays). It is difficult to determine the protolith, but the mineralogy and the texture suggest that it was a gneiss of intermediate to mafic composition.

Most of what is known about the basement lithologies in the Maya block comes from outcrops along its southern margin, where the Chuacús Series is composed of amphibolite, mica schist, gneiss, marble, quartzite, and metavolcanics (e.g., Donnelly et al. 1990). Stratigraphically, this is the oldest sequence of outcrops on the entire Yucatán peninsula. Overlying the Chuacús Series is a thick sedimentary sequence called the Santa Rosa Group. A hiatus separates the Santa Rosa from an overlying sequence of Late Jurassic (Todos Santos) and Cretaceous sediments, which were deposited continuously through the time of the Chicxulub impact event (Donnelly et al. 1990).

A portion of this sequence was sampled in the PEMEX boreholes (López-Ramos 1975). Basement was encountered in Yucatán-1 and Yucatán-4. In the case of Yucatán-1, quartz chlorite schist and an extrusive rhyolite porphyry were found below the Todos Santos red beds. Basement was encountered in two additional boreholes (Basil Jones-1 and Tower Hill-1) in the southern portion of the peninsula (but north of the mountains). In one case, the well bottomed in a schist and, in the other, a granite. These basement lithologies and overlying sediments were intruded by a series of Permian to mid-Triassic granites (Gomberg et al. 1968; Bateson and Hall 1977; Donnelly et al. 1990). Thus, the lithologies seen as clasts in the Yax-1 well are consistent with known basement lithologies in the Maya block, but as yet, direct correlation with specific units is still unclear. In addition, a series of volcanics were produced in the Carboniferous. These volcanics, known as the Bladen volcanics, outcrop in the southern portion of the peninsula. It is not clear if they also occur in the northern part of the peninsula under the site of the Chicxulub impact event. We did not detect any clasts of this material in the Yax-1 core.

Conspicuously missing in the melt-rich breccias of the Yax-1 core are clasts of anhydrite or even secondary anhydrite, both of which were present in Yucatán-2 and Yucatán-6 breccias (Kring et al. 1991; Hildebrand et al. 1991). Estimates for the relative proportion of carbonate and anhydrite in the impact target assemblage are variable. The work of López-Ramos (1975) suggests 49% anhydrite and 45% limestone, but Ward et al. (1995) suggest 30% anhydrite and ~66% dolomite and limestone (see Pierazzo et al. [1998] for a discussion). The megablocks beneath the melt-bearing impactites in the Yax-1 core are 27.4% anhydrite and nearly

72.6% dolomite and limestone (Dressler et al. 2003a). In all cases, the amount of anhydrite in the target assemblage is greater than that inferred from clast populations in the Yax-1 core. Some type of differentiation during the excavation, transportation, and/or deposition of target material must have prevented anhydrite from being deposited at the Yax-1 site. It is possible that the anhydrite may have been a near-surface lithology in the Chicxulub target. Ejecta in the vicinity of the excavation rim should be substantially composed of deep-seated strata, as the rim flap tends to be stratigraphically overturned. For example, the "Wornitzostheim" drill hole just outside the inner ring/excavation rim of the Ries crater displays such dominance of deep-seated strata (e.g., Förstner 1967). It is also possible that the anhydrite had somewhat patchy distribution and was substantially absent in that portion of the crater cavity that gave rise to the Yax-1 deposits. Very generally, the ejection process during crater growth is substantially centrosymmetric and tends to preserve the specific lithological content of the target along radial traverses (Gault et al. 1968; von Engelhardt and Graup 1984).

Source of Impact Melt

Although the impact melt is partially to wholly altered in the Yax-1 borehole, it is clear that it is dominated by silicate compositions, indicating that most of the melt was generated in the silicate-rich basement rather than the 3 km- thick overlying carbonate platform. This is consistent with melt compositions in the Yucatán-6 and Chicxulub-1 boreholes (Kring and Boynton 1992; Sharpton et al. 1992). It is also consistent with observations of melt production at other craters. For example, at the Ries, which is a 24 km- diameter crater produced in a similarly layered target of ~420 m of limestone, sandstone, and shale over a crystalline granitic basement, the melt is also dominated by silicate compositions (e.g., von Engelhardt and Graup 1984), although a small quantity of carbonate melt may have been produced from the Malmiam limestone comprising the target surface (Graup 1999). Carbonate melt has also been described at the Haughton impact site (Osinski and Spray 2001).

Simple scaling calculations suggest that material was excavated from depths of 12 to 14 km and that material was melted and displaced down to depths of 29 to 34 km (Kring 1995). These same calculations suggest that 0.3 to 1 × 10^5 km^3 of melt were generated by the impact event and 2 to 9 × 10^5 km^3 of material was displaced in the Earth's crust, the range reflecting our uncertainty about the impact velocity and, thus, in part, whether the projectile was an asteroid or a relatively higher-velocity comet. More complicated 2D model simulations suggest 0.3 to 0.5 × 10^5 km^3 of melt is produced if the transient crater diameter is ~100 km, with most of the melt coming from the silicate crustal component (Pierazzo et al. 1998), even in an oblique impact, as long as the angle of the trajectory is >~30° (Pierazzo and Melosh 1999). Melt compositions and scaling calculations (Kring 1995), in addition to computer simulations of the impact (Pierazzo et al. 1998; Pierazzo and Melosh 1999), indicate that the mantle was not involved in the melt, so the melt is dominantly produced from silicate basement material in the Maya block. Melt volumes recently estimated using simplified crater geometry suggest smaller melt volumes of 0.1 to 0.2 × 10^5 km^3 (Pope et al. 2004).

As inferred above from the types of basement lithologies in the impactite sequence, the impact melt was probably produced from multiple lithologies. As discussed above, the Yax-1 and Yucatán-6 samples contain unmelted clasts representing sandstone or metaquartzite, shale, granitic lithologies (including a garnet-bearing granite), and at least one mafic lithology. Mixing calculations also suggest that the bulk chemical composition of the melt rock may have been produced from mica schists, carbonates, and/or evaporites in the target (Kring and Boynton 1992). These components were mixed over distances of several to tens of km within a period of a few minutes.

Although the impact melt is dominated by silicate basement sources, contributions from the overlying carbonate platform are evident. Small amounts of immiscible carbonate melts in silicate melt fragments are incorporated in the polymict breccia sequence of Yax-1. In addition, the apatite found in the green melt unit has incorporated S, up to 2 wt% (Table 2), which likely comes from melted anhydrite in the upper 3 km of the target assemblage. It is not clear why we see evidence of a target anhydrite component in the impact melt, but not as clasts in the overlying polymict breccias.

Similar mixing of silicate and carbonate platform target lithologies is apparent from analyses of impact melt spherules deposited several hundred km from the impact site. Sigurdsson et al. (1991a, b), for example, showed that there was a range of impact melt spherule compositions representing a mixture between Ca-carbonate/sulfate lithologies and silicate lithologies. Likewise, oxygen isotope analyses indicated that these melts were produced from isotopically heavy ($\delta^{18}O$ = 14‰) carbonate rocks and isotopically light ($\delta^{18}O$ = 6‰) silicate rocks (Blum and Chamberlain 1992). In addition, primary pyroxene contains an aegerine component, suggesting the uptake during crystallization from the melt, perhaps because the impact-melted protolith was unusually rich in Na (from granitic terranes and possibly halite in evaporites in the overlying carbonate platform) or because of rapid crystallization that permitted the incorporation of elements normally sequestered by feldspar. The aegerine component is also seen in pyroxene in the Yucatán-6 melt (Kring and Boynton 1992).

Unusually Melt-Rich Polymict Breccias

The extraordinary feature of the impactite sequence in the Yax-1 borehole is the high abundance of melt fragments in

the polymict breccias. Some of the breccias are composed almost entirely (up to 84%) of melt fragments (Fig. 6). In the Ries crater, which is the type locality for suevitic melt-bearing breccias, crater suevites (deposited within the transient crater) are only 29% melt fragments, and fall-out suevites (deposited outside the transient crater) are 47% melt fragments (von Engelhardt and Graup 1984). Because the Yax-1 (and Yucatán-6) borehole is located outside the transient cavity of Chicxulub, the better comparison is with the relatively melt-rich fall-out suevites, nonetheless, the abundance of melt fragments in the Chicxulub polymict breccias in Yax-1 are nearly twice as abundant as those in the Ries fall-out suevites.

The large proportion of melt fragments in the Chicxulub melts (up to 84%) may reflect a well-known phenomena: larger impact events produce a larger proportion of melt (and vapor) than smaller craters relative to the total amount of material displaced by the impact event. Scaling with a simple Z-model (Maxwell 1977; as adapted by Melosh [1989]), the total ejected mass $M_{ej} = [(Z - 2)/(Z + 1)]M_{tc}$, where M_{tc} is the mass of the material displaced from the transient crater. For purposes of illustration, we select $Z = 3$, which corresponds to ejecta angles of 45°, leading to $M_{ej} = ¼M_{tc}$. The mass of melt produced by craters of various sizes relative to the mass of material displaced is proportional to $D_{tc}^{0.83}$, where D_{tc} is the diameter of the transient crater (Melosh 1989). The transient crater diameter of Chicxulub appears to be ~100 km (Kring 1995; Morgan et al. 1997). Assuming a final crater diameter of 24 km for the Ries, we calculate a transient crater diameter of 15 km for the Ries (see Kring [1995] for a discussion regarding calculations of transient crater diameters). This corresponds to an "inner ring" at Ries dominated by large, monomict, crystalline basement rocks and lesser polymict basement breccias (Förstner 1967; Abadian 1972). Using these transient crater values and both of the relationships described above, we calculate that the Chicxulub crater should have produced approximately an order of magnitude (factor of 8.5) larger proportion of melt than the Ries crater. In addition to there being more melt in the ejected material in the case of Chicxulub compared to Ries, the amount of melt remaining within the peak ring, relative to the mass of displaced material, is also larger in Chicxulub than in Ries because the proportion of melt relative to the mass of displaced material increases with crater size, exceeding a value of 1 in large craters.

In addition to the relatively large proportion of melt in the Yax-1 breccias, the common juxtaposition, if not intimate mixture, of both jagged fragments and plastically deformed objects, as well as breccia volumes that are clast- or matrix-supported, suggests a much wider range of thermal histories for the Chicxulub melts compared to the Ries suevites. All Ries bombs had substantially cooled below the glass transition temperature, as evidenced by their well- preserved, aerodynamic shapes and by the plethora of shardy, very angular fragments, presumably the result of collisional processes during ballistic deposition (Hörz 1965). Plastic deformation of still viscous objects is substantially absent in most of the Ries suevites. Also, no fine-grained clastic materials adhere to the surfaces of the bombs, whether complete or fractured, suggesting they were essentially rigid objects upon incorporation into the clastic suevite matrix. The only exceptions to this rule at the Ries are somewhat anomalous and rare "red" (oxidized) suevites (e.g., von Engelhardt et al. 1969) that have a molten matrix yet no discrete melt-bombs (albeit abundant, deep-seated clasts). These red suevites are, thus, melt flows that may have breached the confines of the crater rim, in contrast to the more typical fall-out suevite, which underwent a ballistic phase. The melt-rich Chicxulub breccias seem to share properties common to both types of suevites: quenched angular shards and still-viscous melts (or, at least, hot enough to be plastically deformed) were deposited simultaneously, and the surrounding matrix was also either quenched and clastic or sufficiently hot and dense to flow in a viscous, albeit turbulent, fashion. The thermal histories of individual melt volumes at scales of cm to dm were, thus, unusually variable based on previous experience and included plastic, still hot, materials more so than in the classical Ries suevite. This renders the Chicxulub breccias texturally distinct, if not unique, among terrestrial impact formations. The term suevite is, nevertheless, appropriate for units 1 through 4 in the broad sense that they are polymict breccias with impact-melt clasts in a clastic matrix.

Distribution and Thickness of Impact Melt and Melt-Bearing Breccias

Although the proportion of melt in the polymict breccias is large relative to that seen in other impact craters, the total amount of melt in the Yax-1 well (in both the green melt units and overlying breccias) is relatively small. This is true relative to the amount of melt seen elsewhere in the Chicxulub crater and to that seen in other impact craters.

The Chicxulub-1, Sacapuc-1, Yax-1, and Yucatán-6 boreholes indicate that the general impactite stratigraphy within the rim of the crater involves polymict breccias and an underlying impact melt (Fig. 8). Based on analyses of other impact craters, the impact melt is thought to be concentrated within a ~100 km-diameter region of Chicxulub's transient crater, although substantial portions exist in the trough between the peak ring and crater rim, as indicated by the Yax-1 and Yucatán-6 holes. Locally, fragments of ejected melt were found in breccias recovered beyond the crater rim from the Yucatán-2 well (Hildebrand et al. 1991) and are abundant in the continuous cores recovered from the shallow UNAM-5 and -7 boreholes (Sharpton et al. 1999). Breccias also occur within the crater. Using a vertical impact model, it has been estimated that ~25% of the melt produced by the impact was ejected from the transient crater (Kring 1995).

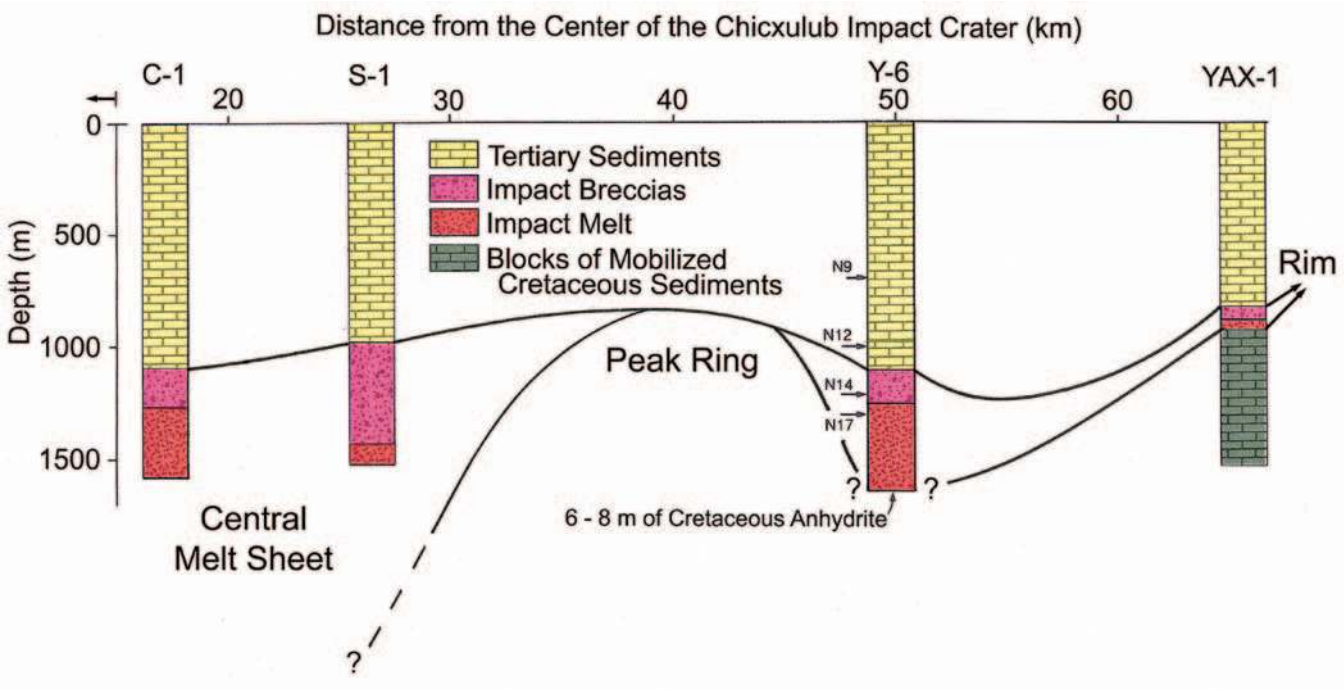

Fig. 8. Lithologies in the Chicxulub crater as revealed in four boreholes arranged in order of distance from the center of the crater. Chicxulub-1 and Sacapuc-1 penetrated the central melt sheet within the peak ring. Yucatán-6 and Yax-1 are interpreted to be in the trough between the peak ring and rim of the crater. Yucatán-6 bottomed in 6 to 8 m of anhydrite, but it is not clear if this is a megablock beneath the impact melt unit or a clast floating in the melt unit. The melt thins considerably between Yucatán-6 and Yax-1. Adapted from Hildebrand et al. (1991).

The thickness of the central melt sheet is still unknown. Models based on geophysical data suggest thicknesses ranging from 3 to 4 km (Sharpton et al. 1993; Pilkington et al. 1994; Snyder et al. 1999; Morgan et al. 2000). The Chicxulub-1 and Sacapuc-1 boreholes indicate that it is at least several hundred m.

The thickness of melt between the peak ring and final crater rim is variable. The Yucatán-6 borehole indicates a melt thickness of 0.38 km and possibly greater. The hole bottomed in 6 to 8 m of anhydrite. It is not clear if this is a megablock beneath the melt (in which case, the melt is 0.38 km thick) or if the anhydrite is a large clast within the melt unit (in which case, the melt is >0.38 km thick). The melt (including the melt-rich breccias) is much thinner in the Yax-1 borehole, which is farther from the center of the crater (~1.2 versus ~1 times the transient crater diameter). It is not clear if the melt at this location is laterally continuous or whether the hole penetrated a pocket of melt. The melt in Yax-1 was encountered at a much shallower depth than in the Yucatán-6 borehole, suggesting the melt in Yax-1 may be ponded on a topographically higher terrace in the modification zone than the Yucatán-6 samples.

The total thickness of the melt-bearing breccias in the Yax-1 cores, some 80 m, is modest compared to the 87 m-thick suevite in the structurally similar Wornitzostheim core, ~3 km outside of the 15 km-diameter inner ring of the Ries (~1.2 times the transient crater diameter) (Förstner 1967), although the patchy distribution of suevites suggests that the thickness can be quite variable (even zero) at any distance. The suevites at the Popigai crater are a few hundred m thick and cover, in essentially continuous fashion, the annulus between the inner and outer ring (Masaitis 1994). The Yax-1 breccias are of modest thickness in comparison to those at these noticeably smaller craters. It is possible that much of the suevitic material is eroded at Chicxulub, yet there is no compelling evidence for large-scale erosion and redeposition of suevite in the core per se. This issue will be discussed further below.

Also, the total thickness of the melt (units 5 and 6) below the polymict breccias, akin to the tagamite/suevite relationships at Popigai (Masaitis 1994; Whitehead et al. 2002), is modest, provided the green melt units even represent such a similar type of melt sheet as the tagamite. If the melt unit is a stratigraphic layer, then that layer is thinner than a layer at a similar distance within Popigai. However, since we only have a core sample, the geometry of the melt unit is not certain. We cannot rule out the possibility that the unit is a displaced block of impact melt that cooled and crystallized somewhere else and was substantially more massive before being moved, which is consistent with the highly cataclastic nature of the unit. In either case, the total melt content of the Yax-1 core is low for a location modestly outside the excavation cavity of a ~180 km-diameter crater.

Penetrating Dikes

The dike at 1398.5 m depth is a clastic breccia that is dominated by dolomite (>95%) and contains minor amounts of limestone (2–4%) and anhydrite (1%). The dike does not resemble mechanically disaggregated host rock and must have originated at some different location (see also Wittmann et al. 2003a). It is not possible to state, however, where this source material resided and how far the brecciated material may have been transported. Limestones, dolomites, and anhydrites occur at vertical distances measured in a few tens of meters, and modest transport distances for the dike materials are, thus, possible, if not likely.

We made a concerted effort to search for crystalline basement clasts in this single dike, yet we found none; this argues for relatively short transport distances. We also searched diligently, yet unsuccessfully, for evidence of melting by either silicate or carbonates. This argues for modest shock stresses during dike formation. Cumulatively, these observations suggest that the dike represents local, sedimentary rocks that were pulverized and subsequently injected into the host during transport and movement of the large, sedimentary megablocks.

Implications for Transport, Deposition, and Modification

In the following, we attempt to synthesize our core observations into a depositional scenario, first addressing the impactites (from bottom to top) and, subsequently, the sedimentary megablocks.

The green melt unit (5) and the underlying basal unit (6) of similar material may be part of a single unit. The primary mineralogy and textures of the green melt in both units are similar, although the basal unit has entrained larger basement clasts and, after deposition, was affected more substantially by carbonate-rich fluids and secondary carbonate precipitation. If the basal unit is part of the same unit as the green melt unit, then the large clasts imply that the melt was deposited in molten form, allowing the large clasts to sink to the bottom of the unit. The mineralogy and textures of the green melt are also similar to the melt unit in the Yucatán-6 borehole, so it may be a thinner portion of a distributed melt unit between the peak ring and final crater rim. This unit may, however, be locally discontinuous because of topography during deposition and subsequent modification of the crater after melt solidification. According to impact simulations (e.g., Pierazzo et al. 1998), the melt was originally consolidated along the walls of the transient crater. It was then either ejected from the transient crater or, as the central peak rose into the atmosphere (Collins et al. 2002), carried upward and then flowed from the central uplift toward the outer portions of the crater before or during the collapse of the central uplift to form the peak ring. Alternatively, the clast-rich unit 6 could have resulted from mechanical disaggregation of the green melt unit while the latter was emplaced as an essentially rigid block of quenched melt. Sufficient pore space was created to promote circulation of carbonate-rich fluids; in this case, the presence of large basement clasts would be fortuitous.

The fine grain size indicates the green melt (unit 5) solidified quickly after being deposited. It was then brecciated and intensely fractured to form a monomict breccia that was subsequently invaded by the same carbonate-rich fluids that permeated unit 6. The green melt unit was solid during the emplacement of the melt-rich breccias of unit 4; that is, the melt cooled substantially while the ejection and deposition of units 1 through 4 was still ongoing. Similarly, rigid and rapidly quenched tagamite melts seem to be present at Popigai before the emplacement of suevites (Whitehead et al. 2002). Even the impact melt at Sudbury (e.g., Therriault et al. 2002) must have had a sufficiently rigid quench zone at the top to mechanically support the deposition and weight of the overlying Onaping formation. These examples show that massive impact melts may quench rather solid melt sheet margins while suevitic ejecta are still being produced and emplaced.

The substantial brecciation of unit 5 seems unique among terrestrial impact melt sheets, although its significance is difficult to determine. The brecciation may have occurred during deposition if the melt solidified as it was still moving laterally outward from the center of the crater. The brecciation could have occurred during the modification stage of crater formation (i.e., within ~10 min of impact), with the solidified melt in place. Alternatively, the entire mass of green melt may represent a displaced block of impact melt from another location and that the intense fracturing occurred during this displacement and/or transport to the new location. Some of the brecciation, however, occurred long after the modification stage, most likely in response to long-term gravitational adjustments because the brecciation has offset veins produced by post-impact hydrothermal activity (Zurcher and Kring 2004).

Units 5 and 6 are quite distinct from the overlaying units 1 through 4 in the Yax-1 cores. The latter are suevite-like, highly polymict breccias composed of a variety of melts and clastic materials. The Yax-1 melts in the polymict breccias cooled quickly to form glassy to microcrystalline textures. Schlieren indicates that melts were being mixed and/or clasts were still being consumed as the melts were solidifying. The size distribution of individual melt objects varies greatly and attests to some thorough physical disaggregation of a large melt volume that was furthermore mixed with clastic material. This pervasive melt-dispersion suggests some form of airborne transport. Rare aerodynamic forms of individual melt objects suggest that some of the material was shaped in free flight, similar to individual melt bombs in the Ries suevites (e.g., Horz 1965; von Engelhardt and Graup 1984). Individual melt volumes followed different trajectories and

cooled at different rates, leading to a mixture of molten and solid particles. These objects also collided with each other to produce shardy, angular fragments and, on occasion, the encasing of some melt by another melt or the draping of a lithic clast by melt. Additional melt fragmentation could have occurred during deposition. Cumulatively, these observations argue for particle collisions in a turbulent environment. The latter may have been set up in mid-air, because the crater-derived melts and clasts were most likely entrained by and mixed with impact-produced rock vapors, including volatiles like H_2O, CO_2, and SO_x that were released from a sedimentary rock portion of the target lithologies. Turbulence was possibly also caused during a ground-hugging debris surge, which was deduced independently by Stöffler et al. (2003a). Transport distances for these melt objects and clasts are readily measured in tens of km from the crater interior to beyond the excavation rim, implying considerable radial momentum of the entire deposit (Oberbeck 1975). It is possible that the freshly deposited melt sheet was reworked by these energetic ejecta to account for the numerous fragments of green melt that are observed in these polymict breccias.

Individual melt objects have grossly similar compositions in these polymict breccias, yet subtle compositional differences may have been overprinted by hydrothermal activity (see Zurcher and Kring 2004). While most of the melt volume is derived from the crystalline basement, some carbonate melts from the sedimentary cover are present as well. This implies incomplete mixing of the entire melt volume at Chicxulub; the textural relationships of silicate and carbonate melts reflect immiscibility of these two melts under the prevailing conditions of rapid quenching. Similar relationships were reported for the Ries suevite and Haughton breccias (Graup 1999; Osinski and Spray 2001). Intimate contact, if not enclosure, by silicate melts seems a prerequisite to preserve the "immiscible" carbonate melt component. The latter is volumetrically subordinate compared to the silicate melts.

The solidified melt in the breccias was shattered and then mixed with carbonate-rich matrix components or was invaded by fluids precipitating secondary calcite. Because portions of the breccias are matrix supported, some carbonate had to be part of the original deposit rather than having been introduced entirely by secondary fluid processes. Consequently, target material from the underlying silicate basement was melted, ejected, and mixed with carbonate material from the upper 3 km of the target lithologies.

In general, the polymict breccias were deposited at relatively low temperatures. The 23 m-thick melt-rich breccia (unit 3) was deposited at temperatures too low (<1000 °C) for all melt fragments to be plastically deformed. Fragments of melt with gas vesicles and small once-glassy melt shards were not flattened nor is there any indication of foliation as in a welded ash flow. Temperatures were also less than a few hundred degrees Celsius because the carbonate-rich matrix did not form a carbonatite-like melt, and micritic carbonate clasts in the carbonate-rich matrix were not resorbed. Thus, while some immiscible carbonate melt co-existed with the silicate melt, the matrix between the solidified silicate melt fragments was solid material.

Units 1 and 2 at the top of the sequence were likely air borne and settled through the atmosphere and, possibly, a water column before coming to rest. The largest particles in the unit, 1 to 2 cm in diameter, could have settled out of the atmosphere within minutes and could have been deposited during or soon after the modification stage of crater formation. It is not clear if the material also settled through a water column, but it would only require a few minutes to a half hour to settle through water depths of ten to five hundred m. These time estimates are based on calculations of single particles of various sizes and appropriate densities settling through the Earth's atmosphere and water columns after the Chicxulub impact event (see Kring and Durda [2002] for details). The mass of particles, however, in the vicinity of the crater and deposited within the crater may have been so large as to cause density flows that surged down toward the ground at much higher velocities, shortening these time scales. Artemieva et al. (2003) calculate similar time scales for 1 to 2 cm particles settling through the atmosphere.

The height of the crater rim should have been great enough to have formed a barrier to the Gulf of Mexico, so fall-back would not have occurred through the atmosphere unless the barrier was breached. If it was breached, the polymict breccias could have been reworked by catastrophic water flows as they were being deposited or soon afterward and possibly before the highest temperature portion of the thermal front from the central melt sheet arrived at the radial distance of the Yax-1 site.

Only the uppermost few meters of the impactite sequence seem to be reworked, leaving few clues to evaluate total erosion yet suggesting an environment that was not very energetic, much less violent. Substantial turbidity currents were possible if the crater cavity was filled by the inrushing, energetic ocean column. However, the outer crater rim was structurally uplifted and covered by ejecta, effectively forming a dam that may have only been breached over geologic time. The oldest alteration minerals in the Yax-1 core suggest that the crater was filled initially by a shallow and occasionally evaporitic lake (Zurcher and Kring 2004). Although rainwater and groundwater flow may have formed the lake, the mineralogy suggests that evaporation led to saline brines. During those times when a lake existed, wave action in the impact basin could have modified the uppermost breccia deposit. The well-bedded Tertiary sediments above the impactites indicate that marine conditions eventually occurred in the crater, so wave action could have modified the uppermost breccia deposit during this period too. The lack of energetic beds in them, however, argue for a relatively

quiescent depositional environment. Despite these hints of post-impact conditions, the style and degree of total erosion is difficult to evaluate from the core materials.

The megablocks beneath the green melt unit potentially could be ejected from the crater (and, thus, transported outward) or represent material that slumped during the modification stage of the crater (and, thus, transported inward) or both, if the material was displaced and deposited before the modification stage began. Micropalaeontological studies are needed to determine whether the entire sediment section from ~900 to 1500 m is stratigraphically coherent or whether it is composed of a few discrete blocks, possibly from various stratigraphic depths. If the section is stratigraphically coherent throughout and is made up of near- surface strata, a strong case could be made for a large slump block. If it is composed of individual blocks from relatively deep-seated sediments, they most likely represent large blocks displaced from within the crater cavity. We note that the inner ring of the Ries is substantially made up of crater-derived crystalline basement blocks, hundreds of meters across, and/or deep-seated, sedimentary materials in the Wornitzostheim core (e.g., Förstner 1967). Stratigraphic assessment of the Yax-1 sediments is, thus, paramount, as relatively shallow or deep source depth(s) would have significant implications. Since the megablocks directly underlie the impact melt breccias in the Yax-1 well, they may correspond well to the gigantic blocks characterizing the inner ring region at Ries, that is, the very blocky materials that compose the "ejecta" layer outside the rim of large-scale excavation cavities and that ultimately grade into more typical (and finer-grained) "Bunte breccia" deposits (Hörz et al. 1983) with increasing radial range. As is the case in the Ries, we expect the late-stage suevite to drape these blocky deposits.

CONCLUSIONS

The Yax-1 core is the first continuous sample through the impactite lithologies within the Chicxulub impact crater. Multiple polymict breccias were deposited on an impact melt unit. Both were deposited on Cretaceous target sediments, which were either ejected outward from the transient cavity and deposited first or else represent blocks of material that slumped inward during the modification stage, during which time the crater grew the dimensions of the transient crater to the final crater diameter. The primary pyroxene and plagioclase mineral assemblage in the melt of Yax-1 resembles that in the Yucatán-6 borehole, including a significant aegerine component in the pyroxene. Both melts were produced largely from silicate crustal lithologies beneath the 3 km-thick carbonate platform that covered the impact site. Small amounts of immiscible carbonate melt in silicate melt fragments have been found in the overlying polymict breccias, and target carbonate formed the solid matrix of those breccias.

The melt in the Yax-1 borehole is located at a shallower depth than that in the Yucatán-6 borehole. It is not yet clear if the melt forms a continuous layer between the two wells (and, thus, in the trough between the peak ring and final crater rim) or whether they represent discontinuous deposits of melts in local catchments.

While the melt unit appears to have been deposited in a molten state, the melt incorporated into the polymict breccias solidified during transport and was fragmented during transport and/or deposition. After being deposited, the melt unit solidified quickly, forming a microcrystalline groundmass. It was then brecciated, either as it continued to move across the surface beyond the transient crater rim (sec to a couple of min), during the modification stage where the crater grew to its final diameter (perhaps 10 min) or in subsequent settling over a much longer time scale.

The proportion of melt (~80%) in the polymict breccias is far greater than that seen previously in impact craters and may occur because the proportion of melt relative to the total amount of displaced material is greater in large impact craters like Chicxulub than in smaller craters.

Although the polymict breccias are unusually rich in melt components, much more so than typical suevites, only ~70 m of melt-rich impactites and ~25 m of massive impact melt was recovered. The total amount of impact melt is, thus, unusually small in this core for a crater the size of Chixculub, some 180 km in diameter. We suggest that the specific core location is on a topographic high, which prevented the deposition of the more massive melt units that can be inferred from other, albeit less complete, drill holes at Chicxulub, as well as from geophysical exploration. It is also possible, although it seems less likely, that only the lower portions of originally more massive deposits were recovered at this specific location.

Acknowledgments–We thank the International Continental Drilling Program and the Chicxulub Scientific Drilling Project team for producing the Yax-1 core. We thank Lutz Hecht, Jo Morgan, and an anonymous reviewer for their helpful comments. The work reported in this paper was supported by NSF Continental Dynamics grant EAR-0126055.

Editorial Handling—Dr. Joanna Morgan

REFERENCES

Abadian M. 1972. Petrographie, Stosswellenmetamorphose und Entstehung Polymikter kristlliner Breccien im Nördlingen Ries. *Contributions to Mineralogy and Petrology* 35:245–262.

Artemieva N. A., Stöffler D., Hecht L., Schmitt R. T., and Tagle R. 2003. Interaction of the ejecta plume and the atmosphere during the deposition of the uppermost suevite layers at the Yax-1 drilling site, Chicxulub, Mexico (abstract #4063). 3rd International Conference on Large Meteorite Impacts. CD-ROM.

Bateson J. H. and Hall I. H. S. 1977. *The geology of the Maya*

Mountains, Belize. Overseas Memoir 3. London: Institute of Geological Sciences. 43 p.

Bell C., Morgan J. V., Hampson G. J., and Trudgill B. 2004. Stratigraphic and sedimentological observations from seismic data across the Chicxulub impact basin. *Meteoritics & Planetary Science* 39:1089–1098.

Blum J. D. and Chamberlain C. P. 1992. Oxygen isotope constraints on the origin of impact glasses from Cretaceous-Tertiary boundary. *Science* 257:1104–1107.

Blum J. D., Chamberlain C. P., Hingston M. P., Koeberl C., Marin L. E., Schuraytz B. C., and Sharpton V. L. 1993. Isotopic comparison of K/T boundary impact glass with melt rock from the Chicxulub and Manson impact structures. *Nature* 364:325–327.

Camargo-Zanoguera A. and Suárez Reynoso G. 1994. Evidencia sismica del crater de impacto de Chicxulub. *Boletín de la Asociación Mexicana de Geofísicos de Exploración* 34:1–28.

Campos-Enríquez J. O., Arzate J. A., Urrutia-Fucugauchi J., and Delgado-Rodríguez O. 1997. The subsurface structure of the Chicxulub crater (Yucatán, México): Preliminary results of a magnetotelluric study. *The Leading Edge* 16:1774–1777.

Claeys P., Heuschkel S., Lounejeva-Baturina E., Sanchez-Rubio G., and Stöffler D. 2003. The suevite of the Chicxulub impact crater. *Meteoritics & Planetary Science* 38:1299–1317.

Collins G. S., Melosh H. J., Morgan J. V., and Warner M. R. 2002. Hydrocode simulations of Chicxulub crater collapse and peak-ring formation. *Icarus* 157:24–33.

Cornejo Toledo A. and Hernandez Osuna A. 1950. Las anomalias gravimetricas en la cuenca salina del istmo, planicie costera de Tabasco, Campeche y Peninsula de Yucatán. *Boletín de la Asociación Mexicana de Geólogos Petroleros* 2:453–460.

Delgado-Rodríguez O., Campos-Enríquez O., Urrutia-Fucugauchi J., and Arzate J. A. 2001. Occam and Bostick 1-D inversion of magnetotelluric soundings in the Chicxulub impact crater, Yucatán, Mexico. *Geofísica Internacional* 40:271–283.

Donnelly T. W., Horne G. S., Finch R. C., and López-Ramos E. 1990. Northern Central America; The Maya and Chortis blocks. In *The Geology of North America, Vol. H—The Caribbean Region,* edited by Dengo G. and Case J. E. Boulder: Geological Society of America. pp. 37–76.

Dressler B. O., Sharpton V. L., Morgan J., Buffler R., Moran D., Smit J., Stöffler D., and Urrutia J. 2003a. Investigating a 65-Ma-old smoking gun: Deep drilling of the Chicxulub impact structure. *Eos Transactions* 84:125, 130.

Dressler B. O., Sharpton V. L., and Marin L. E. 2003b. Chicxulub Yax-1 impact breccias: Whence they come? (abstract #1259). 34th Lunar and Planetary Science Conference. CD-ROM.

Förstner U. 1967. Petrographische Untersuchungen des Suevit an den Bohrungen Deiningen und Wörnitzostheim im Ries von Nördlingen. *Contributions to Mineralogy and Petrology* 15:281–307.

Gault D. E., Quaide W. L., and Oberbeck V. R. 1968. Impact cratering mechanics and structures. In *Shock metamorphism of natural materials,* edited by French B. M. and Short N. M. Baltimore: Mono Book Corp. pp. 87–100.

Gomberg D. M., Banks P. O., and McBirney A. R. 1968. Guatemala: Preliminary zircon ages from central cordillera. *Science* 162: 121–122.

Graup G. 1999. Carbonate-silicate liquid immiscibility upon impact melting: Ries crater, Germany. *Meteoritics & Planetary Science* 34:425–438.

Guzmán E. J. and Mina U. F. 1952. Developments in Mexico in 1952. *Bulletin of the American Association of Petroleum Geologists* 37: 1506–1522.

Hecht L., Kenkmann T., Schmitt R.T., Stöffler D., Tagle R., and Wittmann A. 2003. Petrography, composition, shock metamorphism, and geology of the impact formations of the ICDP drill core Yax-1, Chicxulub crater, Mexico (abstract). *Meteoritics & Planetary Science* 38:A97.

Hildebrand A. R. and Stansberry J. A. 1992. K/T boundary ejecta distribution predicts size and location of Chicxulub crater (abstract). 23rd Lunar and Planetary Science Conference. pp. 537–538.

Hildebrand A. R., Penfield G. T., Kring D. A., Pilkington M., Camargo-Zanoguera A., Jacobsen S., and Boynton W. V. 1991. The Chicxulub crater: A possible Cretaceous-Tertiary boundary impact crater on the Yucatán peninsula, Mexico. *Geology* 19: 867–871.

Hildebrand A. R., Pilkington M., Grieve R. A. F., Robertson P. B., and Penfield G. T. 1992. Recent studies of the Chicxulub crater, Mexico (abstract). 23rd Lunar and Planetary Science Conference. pp. 539–540.

Hildebrand A. R., Pilkington M., Connors M., Ortiz-Aleman C., and Chavez R. E. 1995. Size and structure of the Chicxulub crater revealed by horizontal gravity gradients and cenotes. *Nature* 376: 415–417.

Hörz F. 1965. Untersuchungen an Riesgläsern. *Beiträge zur Mineralogie und Petrologie* 11:621–661.

Hörz R., Horst G., Hüttner R., and Oberbeck V. R. 1977. Shallow drilling in the "Bunte breccia" impact deposits, Ries crater, Germany. In *Impact and explosion cratering,* edited by Roddy D. J., Pepin R. O., and Merrill R. B. New York: Pergamon Press. pp. 425–448.

Hörz F., Ostertag R., and Rainey D. A. 1983. Bunte breccia of the Ries: Continuous deposits of large impact craters. *Reviews of Geophysics and Space Physics* 21:1667–1725.

Kenkmann T., Wittmann A., Scherler D., and Schmitt R. T. 2003a. Deformation features of the Cretaceous units of the ICDP-Chicxulub drill core Yax-1 (abstract #1368). 34th Lunar and Planetary Science Conference. CD-ROM.

Kenkmann T., Wittmann A., Scherler D., and Stöffler D. 2003b. The Cretaceous sequence of the Chicxulub Yax-1 drillcore: What is impact derived? (abstract #4075). 34th Lunar and Planetary Science Conference. CD-ROM.

Kettrup B., Deutsch A., Ostermann M., and Agrinier P. 2000. Chicxulub impactites: Geochemical clues to the precursor rocks. *Meteoritics & Planetary Science* 35:1229–1238.

Kring D. A. 1995. The dimensions of the Chicxulub impact crater and impact melt sheet. *Journal of Geophysical Research* 100:16979–16986.

Kring D. A. and Boynton W. V. 1991. Altered spherules of impact melt and associated relic glass from K/T boundary sediments in Haiti. *Geochimica et Cosmochimica Acta* 55:1737–1742.

Kring D. A. and Boynton W. V. 1992. The petrogenesis of an augite-bearing melt rock in the Chicxulub structure and its relationship to K/T impact spherules in Haiti. *Nature* 358:141–144.

Kring D. A. and Durda D. D. 2002. Trajectories and distribution of material ejected from the Chicxulub impact crater: Implications for postimpact wildfires. *Journal of Geophysical Research* 107, doi: 10.1029/2001JE001532.

Kring D. A., Hildebrand A. R., and Boynton W. V. 1991. The petrology of an andesitic melt rock and a polymict breccia from the interior of the Chicxulub structure, Yucatán, Mexico (abstract). 22nd Lunar and Planetary Science Conference. pp. 755–756.

Kring D. A., Hildebrand A. R., and Boynton W. V. 1994. Provenance of mineral phases in the Cretaceous-Tertiary boundary sediments exposed on the southern peninsula of Haiti. *Earth & Planetary Science Letters* 128:629–641.

Kring D. A., Hörz F., and Zurcher L. 2003. Initial assessment of the excavation and deposition of impact lithologies exposed by the

Chicxulub Scientific Drilling Project, Yaxcopoil, Mexico (abstract #1641). 34th Lunar and Planetary Science Conference. CD-ROM.

López-Ramos E. 1975. Geological summary of the Yucatán peninsula. In *The ocean basins and margins, vol. 3: The Gulf of Mexico and the Caribbean,* edited by Nairn A. E. M. and Stehli F. G. New York: Plenum Press. pp. 257–282.

Masaitis V. L. 1994. Impactites of the Popigai impact crater. In *Large meteorite impacts and planetary evolution,* edited Dressler B. O., Grieve R. A. F., and Sharpton V. L. Special Paper 293. Boulder: Geological Society of America. pp. 153–162.

Maxwell D. E. 1977. Simple Z model of cratering, ejection, and the overturned flap. In *Impact and explosion cratering,* edited by Roddy D. J., Pepin R. O., and Merrill R. B. New York: Pergamon Press. pp. 1003–1008.

Melosh H. J. 1989. *Impact cratering: A geologic process.* New York: Oxford University Press. 245 p.

Morgan J. and Warner M. 1999. Chicxulub: The third dimension of a mutli-ring impact basin. *Geology* 27:407–410.

Morgan J., Warner M., and the Chicxulub Working Group. 1997. Size and morphology of the Chicxulub impact crater. *Nature* 390: 472–476.

Morgan J., Warner M. R., Collins G. R., Melosh H. J., and Christeson G. L. 2000. Peak ring formation in large impact craters: Geophysical constraints from Chicxulub. *Earth & Planetary Science Letters* 183:347–354.

Oberbeck V. R. 1975. The role of ballistic erosion and sedimentation in lunar stratigraphy. *Reviews of Geophysics and Space Physics* 13:337–362.

Osinski G. R. and Spray J. G. 2001. Impact-generated carbonate melts: Evidence from the Haughton structure, Canada. *Earth and Planetary Science Letters* 194:17–29.

Penfield G. T. and Camargo-Zanoguera A. 1981. Definition of a major igneous zone in the central Yucatán platform with aeromagnetics and gravity (abstract). Technical Program, Abstracts and Biographies, Society of Exploration Geophysicists 51st Annual International Meeting. pp. 37.

Penfield G. T. and Camargo-Zanoguera A. 1991. Interpretation of geophysical cross sections on the north flank of the Chicxulub impact structure. Proceedings, 22nd Lunar and Planetary Science Conference. pp. 1051.

Pierazzo E. and Melosh H. J. 1999. Hydrocode modeling of Chicxulub as an oblique impact event. *Earth & Planetary Science Letters* 165:163–176.

Pierazzo E., Kring D. A., and Melosh H. J. 1998. Hydrocode simulation of the Chicxulub impact event and the production of climatically active gases. *Journal of Geophysical Research* 103: 28607–28625.

Pilkington M., Hildebrand A. R., and Ortiz-Aleman C. 1994. Gravity and magnetic field modeling and structure of the Chicxulub crater, Mexico. *Journal of Geophysical Research* 99:131470–13162.

Pope K. O., Kieffer S. W., and Ames D. E. 2004. Emperical and theoretical comparisons of the Chicxulub and Sudbury impact structures. *Meteoritcs & Planetary Science* 39:97–116.

Schmitt R. T., Stöffler D., and Wittmann A. 2003a. Shock metamorphism of impactite lithologies of the ICDP Chicxulub drill core Yax-1 (abstract #1327). 34th Lunar and Planetary Science Conference. CD-ROM.

Schmitt R. T., Wittmann A., and Stöffler D. 2003b. The ICDP drill core Yaxcopoil-1, Chicxulub impact crater, Mexico: Shock metamorphism of the impactite units (794–894 m) (abstract #4061). 34th Lunar and Planetary Science Conference. CD-ROM.

Sharpton V. L., Dalrymple G. B., Marín L. E., Ryder G., Schuraytz B. C., and Urrutia-Fucugauchi J. 1992. New links between the Chicxulub impact structure and the Cretaceous/Tertiary boundary. *Nature* 359:819–821.

Sharpton V. L., Burke K., Camargo-Zanoguera A., Hall S. A., Lee D. S., Marín L. E., Suárez-Reynoso G., Quezada-Muñeton J. M., Spudis P. D., and Urrutia-Fucugauchi J. 1993. Chicxulub multiring impact basin: Size and other characteristics derived from gravity analysis. *Science* 261:1564–1567.

Sharpton V. L., Marín L. E., Carney J. L., Scott L., Ryder G., Schuraytz B. C., Sikora P., and Spudis P. D. 1996. A model of the Chicxulub impact basin based on evaluation of geophysical data, well logs, and drill core samples. In *The Cretaceous-Tertiary event and other catastrophes in Earth history,* edited by Ryder G., Fastovsky D., and Gartner S. Special Paper 307. Boulder: Geological Society of America. pp. 55–74.

Sharpton V. L., Corrigan C. M., Marin L. E., Urrutia-Fucugauchi J., and Vogel T. A. 1999. Characterization of impact breccias from the Chicxulub impact basin: Implications for excavation and ejecta emplacement (abstract #1515). 30th Lunar and Planetary Science Conference. CD-ROM.

Sigurdsson H., D'Hondt S., Arthur M. A., Bralower T. J., Zachos J. C., Van Fossen M., and Channell J. E. T. 1991a. Glass from the Cretaceous/Tertiary boundary in Haiti. *Nature* 349:482–487.

Sigurdsson H., Bonté P., Turpin L., Chaussidon M., Metrich N., Steinberg M., Pradel P., and D'Hondt S. 1991b. Geochemical constraints on source region of Cretaceous/Tertiary impact glasses. *Nature* 353:839–842.

Snyder D. B., Hobbs R. W., and Chicxulub Working Group. 1999. Ringed structural zones with deep roots formed by the Chicxulub impact. *Journal of Geophysical Research* 104:10743–10755.

Stöffler D., Hecht L., Kenkmann T., Schmitt R. T., and Wittman A. 2003a. Properties, classification, and genetic interpretation of the allochthonous impact formations of the ICDP Chicxulub drill core Yax-1 (abstract #1553). 34th Lunar and Planetary Science Conference. CD-ROM.

Stöffler D., Hecht L., Ivanov B. A., Kenkmann T., Salge T., Schmitt R. T., Schönian R., Tagle R., and Wittman A. 2003b. Characteristics of the multi-ring impact basin of Chicxulub, Mexico, as derived from drill core data and numerical modeling (abstract). *Meteoritics & Planetary Science* 38:A126.

Stöffler D., Ivanov B. A., Hecht L., Kenkmann T., Schmitt R. T., Salge T., Schönian R., Tagle R., Weseler S., and Wittman A. 2003c. Origin and emplacement of the impact formations at Chicxulub, Mexico, with special emphasis on the Yax-1 deep drilling (abstract #4092). 3rd International Conference on Large Meteorite Impacts. CD-ROM.

Swisher C. C., III, Grajales-Nishimura J. M., Montanari A., Margolis, S. V., Claeys P., Alvarez W., Renne P., Cedillo-Pardo E., Maurrasse F. J. R., Curtis G. H. 1992. Coeval $^{40}Ar/^{39}Ar$ ages of 65.0 million ago from Chicxulub crater melt rock and Cretaceous-Tertiary boundary tektites. *Science* 257:954–958.

Therriault A. M., Fowler A. D., and Grieve R. A. F. 2002. The Sudbury igneous complex: A differentiated impact melt sheet. *Economic Geology* 97:1521–1539.

Tuchscherer M. G., Reimold W. U., Gibson R. L., and Koeberl C. 2003. Petrographic observations and classification: Impactites from the Yaxcopoil-1 borehole, Chicxulub impact structure, Yucatán peninsula, Mexico (abstract #1310). 34th Lunar and Planetary Science Conference. CD-ROM.

Urrutia-Fucugauchi J., Marin L., and Trejo-Garcia A. 1996. UNAM scientific drilling program of Chicxulub impact structure—Evidence for a 300 km crater diameter. *Geophysical Research Letters* 23:1565–1568.

Vickery A. M., Kring D. A., and Melosh H. J. 1992. Ejecta associated with large terrestrial impacts: Implications for the Chicxulub

impact and K/T boundary stratigraphy (abstract). 23rd Lunar and Planetary Science Conference. pp. 1473–1474.

von Engelhardt W. and Graup G. 1984. Suevite of the Ries crater, Germany: Source rocks and implications for cratering mechanics. *Geologische Rundschau* 73:447–481.

von Engelhardt W., Stöffler D., and Schneider W. 1969. Petrologische Untersuchungen im Ries. *Geologica Bavarica* 6:229–295.

Ward W. C., Keller G., Stinnesbeck W., and Adatte T. 1995. Yucatán subsurface stratigraphy: Implications and constraints for the Chicxulub impact. *Geology* 23:873–876.

Whitehead J., Grieve R. A. F., and Spray J. G. 2002. Mineralogy and petrology of melt rocks from the Popigai impact structure, Siberia. *Meteoritics & Planetary Science* 37:623–647.

Wittmann A., Kenkmann T., Schmitt R. T., and Stöffler D. 2003a. Clastic polymict dikes in the "megablock" sequence of the ICDP-Chicxulub drill core Yax-1 (abstract #1386). 34th Lunar and Planetary Science Conference. CD-ROM.

Wittmann A., Kenkmann T., Schmitt R. T., Hecht L., and Stöffler D. 2003b. Impact melt rocks in the "Cretaceous megablock sequence" of drill core Yaxcopoil-1, Chicxulub crater, Yucatán, Mexico (abstract #4125). 3rd International Conference on Large Meteorite Impacts. CD-ROM.

Zurcher L. and Kring D. A. 2004. Hydrothermal alteration in the core of the Yaxcopoil-1 borehole, Chicxulub impact structure, Mexico. *Meteoritics & Planetary Science* 39:1199–1221

Zurcher L., Kring D. A., Barton M., Dettman D., and Rollog M. 2004. Stable isotope record of post-impact fluid activity in the Chicxulub crater as exposed by the Yaxcopoil-1 borehole, Mexico. Special Paper: Large meteorite impacts. Boulder: Geological Society of America.